Probe particles in odd active viscoelastic fluids: How activity and dissipation determine linear stability

Charlie Duclut [1,2,3,*] Stefano Bo [3,4,†] Ruben Lier,[5,6,‡] Jay Armas,[5,6,§] Piotr Surówka [7,∥] and Frank Jülicher[3,8,9,¶]

[1]*Laboratoire Physique des Cellules et Cancer (PCC), CNRS UMR 168, Institut Curie, Université PSL, Sorbonne Université, 75005 Paris, France*

[2]*Université Paris Cité, Laboratoire Matière et Systèmes Complexes (MSC), UMR 7057 CNRS, F-75205 Paris, France*

[3]*Max Planck Institute for the Physics of Complex Systems, 01187 Dresden, Germany*

[4]*Department of Physics, King's College London, London WC2R 2LS, United Kingdom*

[5]*Institute for Theoretical Physics, University of Amsterdam, 1090 GL Amsterdam, The Netherlands*

[6]*Dutch Institute for Emergent Phenomena (DIEP), University of Amsterdam, 1090 GL Amsterdam, The Netherlands*

[7]*Department of Theoretical Physics, Wrocław University of Science and Technology, 50-370 Wrocław, Poland*

[8]*Center for Systems Biology Dresden, Pfotenhauerstrasse 108, 01307 Dresden, Germany*

[9]*Cluster of Excellence Physics of Life, TU Dresden, 01307 Dresden, Germany*

Odd viscoelastic materials are constrained by fewer symmetries than their even counterparts. The breaking of these symmetries allows these materials to exhibit different features, which have attracted considerable attention in recent years. Immersing a bead in such complex fluids allows for probing their physical properties, highlighting signatures of their oddity and exploring the consequences of these broken symmetries. We present the conditions under which the activity of an odd viscoelastic fluid can give rise to linear instabilities in the motion of the probe particle, and we unveil how the features of the probe particle dynamics depend on the oddity and activity of the viscoelastic medium in which it is immersed.

I. INTRODUCTION

Chiral two-dimensional materials break parity symmetry and display transport phenomena characterized by tensors that are odd under index exchange. Such odd systems attract considerable interest from a broad range of communities. These include soft active matter, statistical physics and biological physics [1–15], fluid dynamics [16–22], complex materials [23–27], electron fluids [28–30], and topological waves [31–34]. Recent experiments have begun measuring odd systems [6,11,30,35]. One of these odd phenomena is odd elasticity [11,23]. Odd elastic solids can perform net work under quasistatic cycles, implying that they are active materials, as such phenomena can only occur in the presence of a constant energy injection at the microscopic level. Such energy injection, if not properly dissipated, can give rise to linear instabilities [23,25]. Complex materials that exhibit elastic properties at short times and fluidlike ones at long times are called viscoelastic. Odd viscoelastic systems were first discussed in [12] in the context of active matter and recently shown to exist also in a passive context, provided that certain thermodynamic constraints are obeyed [3].

A powerful method of probing the physical properties of a fluid is to observe the motion of a probe particle immersed in it [36–38]. This is even more important for active odd viscoelastic materials, for the following reasons: First, the response contains signatures of the odd nature of the material, such as odd lift forces orthogonal to the probe's motion [39,40]. Second, the viscoelastic nature of the system makes the response in time to instantaneous external perturbations nontrivial [41]. Third, activity can give rise to sustained motion of the probe particle and, potentially, instability in the response to perturbations (see, e.g., Ref. [42]).

In this work, we shed light on these three points by looking at the motion of a passive probe particle in an active odd viscoelastic fluid (see Fig. 1). For symmetry reasons, isotropic odd fluids only exist in two dimensions [43], and therefore we focus on this case in this paper, although our methods could be applied in higher dimensions. Moreover, lift forces vanish in incompressible odd fluids [18] when no-slip boundary conditions hold [44], but they can exist in compressible fluids [39]. To assess odd viscoelastic responses in a generic framework, we therefore consider in the following a weakly compressible fluid, and odd lift responses will also be discussed.

First, we derive the material properties of such fluid from Onsager's theory, and we show that activity introduces interesting physics by breaking the Onsager-symmetry

*charlie.duclut@curie.fr
†stefano.bo@kcl.ac.uk
‡r.lier@uva.nl
§j.armas@uva.nl
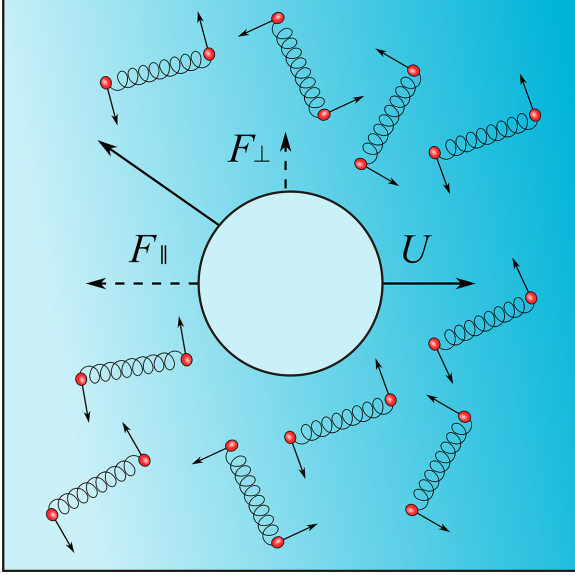∥piotr.surowka@pwr.edu.pl
¶julicher@pks.mpg.de

FIG. 1. Schematic picture of a probe particle moving with velocity U in an odd viscoelastic fluid, experiencing a drag force $F_\parallel$ and a lift force $F_\perp$.

and thermodynamic inequalities that otherwise constrain the stress-strain relations. We then unveil the conditions that grant the stability of the motion of the probe particle when it is embedded in an active fluid. After confirming that a probe in a passive system has a stable trajectory, i.e., its velocity decays at long times, we show that, within our linear approach, there exists an intermediate regime where the probe motion through an active system is still stable. For larger activities, a probe that is subjected to an external force at an initial time becomes linearly unstable. We also focus on the signatures of oddity, which can be seen in the dynamics of the probe. We observe that odd viscoelastic terms promote long-lasting oscillations during the relaxation process after an instantaneous perturbation. These findings provide tools to assess the degree of oddity of a material by studying the motion of a probe inserted in it.

II. PROBE PARTICLE IN AN ACTIVE ODD VISCOELASTIC FLUID

A. Constitutive equations for the fluid

In this section, we discuss the material properties of the two-dimensional odd viscoelastic fluid in which the probe particle moves. For this purpose, we start with the total stress tensor $\underline{\underline{\sigma}}^{\text{tot}}$, which enters the momentum balance equation as

$$\partial_t \mathbf{g} - \nabla \cdot \underline{\underline{\sigma}}^{\text{tot}} = \mathbf{f}^{\text{ext}}. \tag{1}$$

We have introduced the momentum $\mathbf{g} = \rho \mathbf{v}$, with ρ and v_i the fluid mass density and velocity, respectively, and $\mathbf{f}^{\text{ext}}$ is an external force density. Mass density is conserved and obeys $\partial_t \rho + \nabla \cdot (\rho \mathbf{v}) = 0$. The total stress $\underline{\underline{\sigma}}^{\text{tot}}$ can be decomposed into

$$\underline{\underline{\sigma}}^{\text{tot}} = -\rho \mathbf{v} \otimes \mathbf{v} - P \mathbb{1} + \underline{\underline{\sigma}}^{\text{s}} + \underline{\underline{\sigma}}^{\text{a}}, \tag{2}$$

where $\otimes$ is the outer product and $\mathbb{1}$ is the identity tensor. The tensor $\underline{\underline{\sigma}}^{\text{s}}$ is the symmetric deviatoric stress, which incorporates viscoelastic contributions, and $\underline{\underline{\sigma}}^{\text{a}}$ is the antisymmetric part of the stress [45].

For a *passive* odd viscoelastic fluid, the constitutive equations for the stress $\underline{\underline{\sigma}}^{\text{s}}$ and strain $\underline{u}$ tensors are found to be (see Appendix A for more details, also on $\underline{\underline{\sigma}}^{\text{a}}$)

$$\underline{\underline{\sigma}}^{\text{s}} = \boldsymbol{\nu}^{\text{p}} : \underline{\underline{\sigma}}^{\text{el}} + 2\boldsymbol{\eta}^{\text{p}} : \underline{v}, \tag{3a}$$

$$\frac{\mathrm{D}\underline{\underline{u}}}{\mathrm{D}t} = -\boldsymbol{\gamma}^{\text{p}} : \underline{\underline{\sigma}}^{\text{el}} + \boldsymbol{\nu}^{\text{p}} : \underline{v}, \tag{3b}$$

where $\mathrm{D}/\mathrm{D}t$ is the corotational derivative, and $\underline{v} = [\nabla \underline{v} + (\nabla \underline{v})^\top]/2$ is the symmetric part of the velocity gradient tensor. The elastic stress $\underline{\underline{\sigma}}^{\text{el}}$ results from the local strain $\underline{u}$ within the material and is obtained as $\underline{\underline{\sigma}}^{\text{el}} = \delta f / \delta \underline{u}$, where f denotes the free-energy density.

The objects $\boldsymbol{\nu}^{\text{p}}$, $\boldsymbol{\eta}^{\text{p}}$, and $\boldsymbol{\gamma}^{\text{p}}$ in Eq. (3) are four-tensors that are isotropic and symmetric under the exchange of the first two as well as the last two indices, i.e., for a general four-tensor $\boldsymbol{\beta}$ we have $\beta_{ijkl} = \beta_{jikl} = \beta_{ijlk}$. Such a general tensor can thus be characterized in two dimensions by a shear β_{s}, bulk β_{b}, and odd β_{o} coefficient (more details on the tensor notation can be found in Appendix B). The four-tensor $\boldsymbol{\eta}^{\text{p}}$ in Eq. (3) corresponds to all viscous corrections, whereas $\boldsymbol{\gamma}^{\text{p}}$ incorporates plasticity or strain relaxation.

As a consequence of Onsager symmetry (see Appendix C for its derivation for odd materials), the same four-tensor $\boldsymbol{\nu}^{\text{p}}$ relates the deviatoric stress to elastic stress and the strain rate to the velocity gradient. We emphasize that the odd coefficient $\nu_{\text{o}}^{\text{p}}$ is responsible for a *passive* and transient odd elasticity [3] (while steady-state odd elasticity cannot be passive [23]). Finally, to qualify as a passive material, the coefficients entering the four-tensors of Eq. (3) must satisfy [3]

$$\eta_{\text{s}}^{\text{p}}, \eta_{\text{b}}^{\text{p}}, \gamma_{\text{s}}^{\text{p}}, \gamma_{\text{b}}^{\text{p}} \geqslant 0, \quad 2\eta_{\text{s}}^{\text{p}}\gamma_{\text{s}}^{\text{p}} \geqslant \left(\nu_{\text{o}}^{\text{p}}\right)^2, \tag{4}$$

as dictated by the positivity of the entropy production rate.

In this paper, we go beyond passive systems and include activity. This can be done in the Onsager framework, in the spirit of active gel models, by introducing fuel consumption at the microscopic level (see, e.g., Refs. [45,46]). Fuel consumption can be represented by adding a thermodynamic flux, the scalar reaction rate r, and its associated thermodynamic force $\Delta\mu$, which is the chemical potential difference of a chemical reaction, to the description. Since it is an additional thermodynamic force, one should supplement Eq. (3) with terms proportional to $\Delta\mu$, where, by symmetry, the proportionality factor should be a rank-2 tensor. We thus add the active contributions $\Delta\mu(\boldsymbol{\zeta}^{(1)} : \underline{\underline{\sigma}}^{\text{el}} + 2\boldsymbol{\zeta}^{(2)} : \underline{v})$ to Eq. (3a) and $\Delta\mu(-\boldsymbol{\zeta}^{(3)} : \underline{\underline{\sigma}}^{\text{el}} + \boldsymbol{\zeta}^{(4)} : \underline{v})$ to Eq. (3b). In an Onsager framework, the thermodynamic forces (here $\Delta\mu$, $\underline{\underline{\sigma}}^{\text{el}}$, and $\underline{v}$) are considered small, and the expansion of the thermodynamic fluxes as a function of the forces is kept to the lowest order. This means that the $\Delta\mu\underline{\underline{\sigma}}^{\text{el}}$- and $\Delta\mu\underline{v}$-terms are second order, and one would therefore naively think that these terms should be neglected. However, as we will show in the rest of the paper, because these contributions are not bound by passivity constraints, even a small contribution can destabilize the odd viscoelastic model, and therefore to correctly capture the

qualitative behavior of the active viscoelastic system we must retain them.

Finally, the constitutive equation for the stress $\underline{\underline{\sigma}}^{\text{s}}$ and strain $\underline{\underline{u}}$ tensors characterizing two-dimensional odd active viscoelastic fluids read

$$\underline{\underline{\sigma}}^{\text{s}} = \boldsymbol{\nu} : \underline{\underline{\sigma}}^{\text{el}} + 2\boldsymbol{\eta} : \underline{\underline{v}}, \tag{5a}$$

$$\frac{\text{D}\underline{\underline{u}}}{\text{D}t} = -\boldsymbol{\gamma} : \underline{\underline{\sigma}}^{\text{el}} + \boldsymbol{\nu}' : \underline{\underline{v}}, \tag{5b}$$

where we have defined the active rank-four tensors $\boldsymbol{\nu} = \boldsymbol{\nu}^{\text{p}} + \Delta\mu\boldsymbol{\zeta}^{(1)}$, $\boldsymbol{\eta} = \boldsymbol{\eta}^{\text{p}} + \Delta\mu\boldsymbol{\zeta}^{(2)}$, $\boldsymbol{\gamma} = \boldsymbol{\gamma}^{\text{p}} + \Delta\mu\boldsymbol{\zeta}^{(3)}$, and $\boldsymbol{\nu}' = \boldsymbol{\nu}^{\text{p}} + \Delta\mu\boldsymbol{\zeta}^{(4)}$.

Note that the effect of activity ($\Delta\mu \neq 0$) is twofold: (i) it can break the symmetry of the Onsager matrix, which happens whenever $\boldsymbol{\nu}' \neq \boldsymbol{\nu}$. For this reason, $\boldsymbol{\nu}$ and $\boldsymbol{\nu}'$ can be understood as a nonequilibrium and nonreciprocal generalization of classical elasticity; or (ii) it can break the semidefiniteness of the Onsager matrix.

When discussing the stability of the probe in Secs. III and IV, we we will make use of the passive limit for the generalized tensor objects, which can be imposed by setting[1]

$$2\eta_{\text{s}}\gamma_{\text{s}} \geqslant \nu_{\text{o}}^2, \quad \boldsymbol{\nu} = \boldsymbol{\nu}', \tag{6}$$

and where $\eta_{\text{s}}, \eta_{\text{b}}, \gamma_{\text{s}}, \gamma_{\text{b}} \geqslant 0$ is always satisfied provided $\Delta\mu$ is small.

B. Jeffreys model for the odd viscoelastic fluid

Having in mind the description of a probe particle embedded in a viscoelastic fluid, we now show how Eq. (5) leads to an odd Jeffreys model [47,48]. We consider a material with linear elastic properties, and first use the identity

$$\underline{\underline{\sigma}}^{\text{el}} = 2\boldsymbol{G} : \underline{\underline{u}}, \tag{7}$$

where $\boldsymbol{G}$ is the four-tensor of elastic moduli. Since Eq. (7) is derived from free energy, it is not possible to have an odd elastic modulus [23] and thus $G_{\text{o}} = 0$. Note, however, that odd linear couplings between the stress and the strain are present in Eq. (5), and correspond to nonequilibrium corrections derived following Onsager's theory.

Solving for the strain $\underline{\underline{u}}$, we find that the constitutive equations (5) can be rewritten as

$$\left(\boldsymbol{I} + \boldsymbol{\tau}_1 \frac{\text{D}}{\text{D}t}\right) : \underline{\underline{\sigma}}^{\text{s}} = 2\boldsymbol{\eta}^{\text{eff}}\left(\boldsymbol{I} + \boldsymbol{\tau}_2 \frac{\text{D}}{\text{D}t}\right) : \underline{\underline{v}}, \tag{8}$$

where $\boldsymbol{I}$ is the rank-4 identity and where we have used the fact that the contraction of an odd isotropic rank-4 tensor with a rank-2 tensor commutes with taking the corotational time derivative. We have moreover defined $\boldsymbol{\tau}_1 = \boldsymbol{\gamma}^{-1}\boldsymbol{G}^{-1}/2$, $\boldsymbol{\eta}^{\text{eff}} = \boldsymbol{\eta} + \boldsymbol{\nu}\boldsymbol{\gamma}^{-1}\boldsymbol{\nu}'/2$, and $\boldsymbol{\tau}_2 = (\boldsymbol{\eta}^{\text{eff}})^{-1}\boldsymbol{\tau}_1\boldsymbol{\eta}$, where four-tensor algebra is given in Appendix B. Equation (8) describes an odd active Jeffreys model, that is, a viscoelastic fluid with two (odd) dampers and one (odd) elastic spring, as depicted
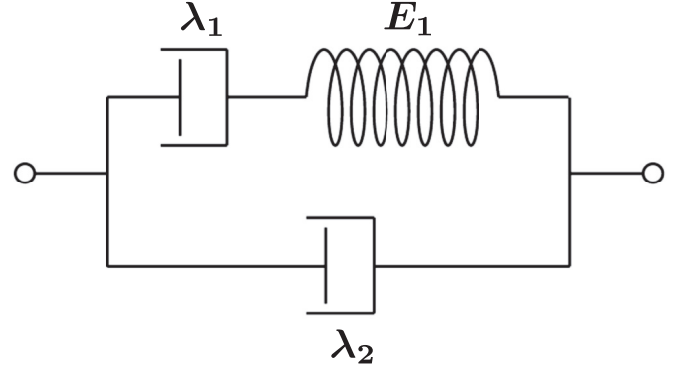

FIG. 2. Circuit representation of the odd Jeffreys model given in Eq. (8) including dampers ($\boldsymbol{\lambda}_{1,2}$) and an elastic spring ($\boldsymbol{E}_1$). Each element of this representation has odd and even contributions, and can be represented as a rank-4 tensor (see the text for details). The relation between the rank-4 tensors appearing in Eq. (8) and the circuit rank-4 tensors is given by $\boldsymbol{\lambda}_1 = \boldsymbol{\eta}$, $\boldsymbol{E}_1 = \boldsymbol{\nu}\boldsymbol{G}\boldsymbol{\nu}'$, and $\boldsymbol{\lambda}_2 = \boldsymbol{\nu}\boldsymbol{\gamma}^{-1}\boldsymbol{\nu}'/2$.

schematically on Fig. 2. Furthermore, one consequence of the thermodynamic constraint (4) is that an odd Maxwell model, for which τ_2 in Eq. (8) vanishes, cannot be passive [3]. Similarly, the odd Kelvin-Voigt limit ($\gamma_{\text{s}} \to 0$, $\nu_{\text{o}} \neq 0$) is also forbidden by thermodynamics in the absence of fuel consumption.

In Laplace space, dropping the (nonlinear) vorticity contributions to the corotational time derivative, we can write the constitutive relation of the active odd Jeffreys model (8) as [36,49]

$$\underline{\underline{\sigma}}^{\text{s}}(s) = 2\boldsymbol{A}(s) : \underline{\underline{v}}(s), \tag{9}$$

where $\boldsymbol{A}(s) = \boldsymbol{\eta} + (\boldsymbol{I} + s\boldsymbol{\tau}_1)^{-1} \cdot \boldsymbol{\nu}\boldsymbol{\gamma}^{-1}\boldsymbol{\nu}'/2$ contains the shear and odd components

$$A_{\text{s}}(s) = \eta_{\text{s}} + \frac{\left(\gamma_{\text{s}} + \frac{s}{2G_{\text{s}}}\right)(\nu_{\text{s}}\nu_{\text{s}}' - \nu_{\text{o}}\nu_{\text{o}}') + \gamma_{\text{o}}(\nu_{\text{o}}\nu_{\text{s}}' + \nu_{\text{o}}'\nu_{\text{s}})}{2\{\gamma_{\text{o}}^2 + [\gamma_{\text{s}} + s/(2G_{\text{s}})]^2\}}, \tag{10a}$$

$$A_{\text{o}}(s) = \eta_{\text{o}} + \frac{\left(\gamma_{\text{s}} + \frac{s}{2G_{\text{s}}}\right)(\nu_{\text{o}}\nu_{\text{s}}' + \nu_{\text{o}}'\nu_{\text{s}}) - \gamma_{\text{o}}(\nu_{\text{s}}\nu_{\text{s}}' - \nu_{\text{o}}\nu_{\text{o}}')}{2\{\gamma_{\text{o}}^2 + [\gamma_{\text{s}} + s/(2G_{\text{s}})]^2\}}, \tag{10b}$$

$$A_{\text{b}}(s) = \eta_{\text{b}} + \frac{\nu_{\text{b}}\nu_{\text{b}}'}{2[s/(2G_{\text{b}}) + \gamma_{\text{b}}]}, \tag{10c}$$

where we have introduced the Laplace transform $\mathcal{L}[h(t)](s) = h(s) = \int_0^\infty dt\, e^{-st}h(t)$ (using the same notation for the function and its transform). We will refer to the coefficients in Eq. (10) as Laplace viscosities, as they can be seen as viscoelastic generalizations of viscosity in the Laplace domain.

To illustrate the physical meaning of the Laplace viscosity tensor $\boldsymbol{A}(s)$, let us consider an even material with $\boldsymbol{\nu} = \boldsymbol{\nu}'$. In this case, A_{s} turns into

$$\tilde{A}_{\text{s}}(s) = \eta_{\text{s}} + \frac{\nu_{\text{s}}^2}{2\gamma_{\text{s}} + s/G_{\text{s}}}, \tag{11}$$

which corresponds to the usual Jeffreys model, which is viscous at very short timescales with viscosity $\lim_{s\to\infty}\tilde{A}_{\text{s}}(s) = \eta_{\text{s}}$, elastic on intermediate timescales, and again viscous at

long timescales with viscosity $\lim_{s\to 0} \tilde{A}_s(s) = \eta_s + \frac{\nu_s^2}{2\gamma_s}$. Note that the only role of activity, in this case, is to modify the values of the different parameters compared to their passive counterparts, while the physics is qualitatively unchanged.

From this simple discussion, we understand that the odd viscoelastic Jeffreys model [Eqs. (9) and (10)] (i) is also characterized by a viscous, fluidlike behavior at short and long timescales; (ii) has three characteristic timescales in the shear and odd sectors, and two in the bulk sector; (iii) can have qualitative differences compared to the even Jeffreys model since the sign of some effective parameters is not fixed (for instance, the term $\nu_s \nu_s' - \nu_o \nu_o'$ in A_s).

C. Probe particle

We now study the motion of a probe particle dragged in the viscoelastic fluid with constitutive equation (9). As discussed in the Introduction, isotropic odd materials only exist in two dimensions, and we thus focus on this case in the following. A natural setting for a two-dimensional viscoelastic fluid is to consider a thin layer of such a fluid at the interface between two bulk (even) fluids, for instance water and air [39,40]. For simplicity, we consider this layer to be flat and infinitely thin, such that the odd fluid can be described effectively as two-dimensional.

The probe particle velocity $\mathbf{U}(t)$ corresponding to an applied time-dependent force $\mathbf{F}(t)$ can be computed using Laplace transforms as

$$U_i(t) = \mathcal{L}^{-1}[\mathbb{M}_{ij}(s)F_j(s)](t), \tag{12}$$

where Latin indices correspond to Cartesian coordinates, and a summation over repeated indices is implied, and with $\mathcal{L}^{-1}[h(s)](t)$ the inverse Laplace transform. The response matrix $\mathbb{M}_{ij}(s)$ can be understood as a viscoelastic and therefore s-dependent generalization of the drag and lift coefficients for a purely viscous fluid. For simplicity, we consider only the translational degrees of freedom of the probe, noticing that in the incompressible limit and for rigid probes there is no odd viscosity-induced torque [18].

To obtain the response matrix $\mathbb{M}_{ij}(s)$ of an odd viscoelastic fluid, we first linearize to first order in v_i and $\delta\rho = \rho - \rho_0$ the momentum and mass conservation equations. To discuss weakly compressible fluids, we need to specify an equation of state for the pressure, which at first order in $\delta\rho$ reads $P = \frac{\delta\rho}{\psi\rho_0}$, where ψ is the compressibility. Note that the incompressible case, for which the pressure is independent of density, is recovered by taking the limit $\psi \to 0$ in the response matrix $\mathbb{M}_{ij}(s)$. Then, using the constitutive equation (9), we obtain the following coupled linearized equations:

$$\rho_0 s v_i = A_s(s)\partial_k\partial_k v_i + A_b(s)\partial_i\partial_k v_k$$
$$+ A_o(s)\varepsilon_{ij}\partial_k\partial_k v_j - \frac{1}{\psi\rho_0}\partial_i\delta\rho + f_i^{\text{ext}}, \tag{13a}$$

$$s\delta\rho = -\rho_0\partial_k v_k. \tag{13b}$$

Using a spatial Fourier transform with the convention $h(\mathbf{x}) = \frac{1}{(2\pi)^2}\int d^2\mathbf{k}\, h(\mathbf{k})e^{i\mathbf{k}\cdot\mathbf{x}}$, Eq. (13) can then be rewritten in matrix form:

$$\mathcal{G}_{ij}v_j = f_i^{\text{ext}}, \tag{14}$$

with $\mathcal{G}_{ij}$ given by [39,40]

$$\mathcal{G}_{ij} = \hat{k}_i\hat{k}_j\left[s\rho_0 + \left(A_s(s) + A_b(s) + \frac{1}{\psi s}\right)k^2\right]$$
$$+ (\delta_{ij} - \hat{k}_i\hat{k}_j)[s\rho_0 + A_s(s)k^2] + \varepsilon_{ij}A_o(s)k^2, \tag{15}$$

where $k = \sqrt{k_i k_i}$ and $\hat{k}_i = k_i/k$. Having formulated the linearized equations for a given Laplace frequency and Fourier wave vector, we can then use the shell localization approach [39,49,50] to obtain the linear response for a rigid disk-shaped probe particle moving in the viscoelastic fluid. When no-slip boundary conditions hold, the shell localization approach prescribes that, upon identifying the probe particle velocity $U_i(s)$ with $v_i(|\mathbf{x}| = 0, s)$, the response matrix is given by (more details are in Appendix D)

$$\mathbb{M}_{ij}(s) = \frac{1}{(2\pi)^2}\int_0^{2\pi}d\theta\int_0^\infty dk\,kJ_0(ak)\mathcal{G}_{ij}^{-1}(\mathbf{k},s), \tag{16}$$

where θ is the angle of the wave vector, a is the disk radius, and $J_0(z)$ is the zeroth Bessel function of the first kind.

For concreteness, and before discussing in detail the drag and lift responses of a probe in an odd active viscoelastic fluid, let us first relate this expression, Eq. (16), to the well-known drag in an incompressible, even, purely viscous fluid in two dimensions. In this case, the response matrix is diagonal and can be written as $\mathbb{M}_{ij}^{\text{simp}}(s) = M_\parallel^{\text{simp}}(s)\delta_{ij}$, where the drag coefficient reads $M_\parallel^{\text{simp}}(s) = \frac{1}{4\pi\eta_s}K_0(\sqrt{\tau_0 s})$, with $\tau_0 = \rho_0 a^2/\eta_s$, and K_0 is the zeroth modified Bessel function of the second kind. This expression can then be expanded in series of the Laplace frequency s, leading to

$$M_\parallel^{\text{simp}}(s) = \frac{-1}{4\pi\eta_s}\left(\log\frac{\sqrt{s\tau_0}}{2} + \gamma_{\text{EM}}\right) + O(s\tau_0), \tag{17}$$

where γ_{EM} is the Euler-Mascheroni constant. This last expression shows the expected divergence of the drag at vanishing frequency, a signature of the Stokes paradox in two dimensions.

III. LINEAR STABILITY OF A PROBE PARTICLE IN AN ODD ACTIVE VISCOELASTIC FLUID

A. General case

Active viscoelastic fluids can give rise to sustained motion. Therefore, the response of a probe placed into the medium after an initial perturbation does not necessarily decay to zero. At the level of linear response, such sustained motion is signaled by instability, which appears in the long-time behavior of the probe velocity given by Eq. (12). Without loss of generality, we consider an instantaneous perturbation applied at $t = 0$, such that $\mathbf{F}(t) \propto \delta(t)$, where $\delta(t)$ is the Dirac delta function. The velocity of the probe after this initial perturbation is given by

$$U_i(t) = \frac{1}{2\pi i}\int_{\Gamma-i\infty}^{\Gamma+i\infty}ds\,e^{st}\int\frac{d^2\mathbf{k}}{(2\pi)^2}m_i(\mathbf{k},s)J_0(k), \tag{18}$$

where $m_i(\mathbf{k},s) = \mathcal{M}_{ij}(\mathbf{k},s)F_j$, and Γ is a real number such that the integral over s is convergent. To discuss stability, we need not focus on the precise expression of the velocity, but we make the crucial point that $m_i(\mathbf{k},s)$ is a rational fraction

in s. This implies that the long-term behavior of the velocity, and therefore the probe stability, is determined by the sign of the real part of the poles in s of m_i:

$$\mathrm{Re}(s_\ell^*(\mathbf{k})) \leqslant 0 \qquad \forall \ell, \ \forall \mathbf{k}, \qquad (19)$$

where $s_\ell^*(\mathbf{k})$ is a pole of m_i; see Appendix E for details. In the general case of an odd compressible viscoelastic fluid, the poles of m_i are roots of a high-order polynomial, which makes further analytical discussion difficult. Nonetheless, Eq. (19) provides a simple and powerful criterion to determine the probe stability that can easily be used numerically. In the following, Sec. III B, we discuss the case of an incompressible fluid, where the analytical discussion regarding stability can be continued.

Note finally that in the regions of the parameter space where the inequality (19) is not satisfied, the motion of a probe is not linearly stable: the passive probe is therefore set into motion by the active viscoelastic fluid. To obtain physical solutions at longer times, nonlinear corrections must then be added to the description. The discussion of the form that these nonlinear corrections should take and their impact on the probe dynamics is left for future work.

B. Stability of probe motion in the incompressible limit

To continue our stability analysis while keeping the technicalities to a minimum, we now restrict ourselves to the incompressible case. In this simpler case, odd lift effects are absent [17,39], the tensor $\mathcal{M}_{ij}$ is proportional to the identity, and the probe particle stability is determined by the poles of

$$r(k, s) = \frac{1}{4\pi\eta_s} \frac{ak J_0(ak)}{\tau_0 s + (ak)^2 A_s(s)/\eta_s}, \qquad (20)$$

with $\tau_0 = \rho_0 a^2/\eta_s$. As shown in Appendix E, these poles in the complex plane correspond to the roots of a third-order polynomial, and stability can be discussed analytically. We first discuss the simpler case in which Onsager symmetry is enforced.

Onsager-symmetric fluid. We can take $\boldsymbol{\nu} = \boldsymbol{\nu}'$, and stability is ensured iff

$$4\gamma_s\eta_s - \nu_o^2 + \nu_s^2 > 0, \qquad (21a)$$

$$2\eta_s\gamma_o^2 + 2\gamma_o\nu_o\nu_s + \gamma_s\big(2\gamma_s\eta_s - \nu_o^2 + \nu_s^2\big) > 0, \qquad (21b)$$

and

$$\Delta < 0 \text{ or } \begin{cases} \Delta \geqslant 0 \quad \text{and} \\ \gamma_s\big(\nu_s^2 - \nu_o^2\big) - 2\gamma_o\nu_o\nu_s + 8\eta_s\gamma_s^2 < 0 \end{cases} \qquad (21c)$$

with $\Delta = b_1^2 - 4b_0 b_2$, where $b_0 = 4G_s^3\gamma_s(\gamma_s^2 + \gamma_o^2)$, $b_1 = G_s^2[\gamma_s(8\gamma_s\eta_s - \nu_o^2 + \nu_s^2) - 2\gamma_o\nu_o\nu_s]/(\tau_0\eta_s)$, and $b_2 = G_s(4\gamma_s\eta_s - \nu_o^2 + \nu_s^2)/(\tau_0^2\eta_s)$.

It is important to note that if the thermodynamics constraint (6) holds, all the conditions of Eq. (21) are satisfied and the system is always stable at long-time, as expected. Constraint (21b) coincides with the condition for the stability of a general odd viscoelastic fluid, which we derived in Ref. [3] by considering the stability of perturbative modes. We also note that the constraint (21c) depends on the mass density ρ_0 (through τ_0), whereas the other constraints Eqs. (21a) and (21b) only depend on viscoelastic coefficients.

For concreteness, we show in Fig. 3 stability diagrams of a probe immersed in an odd incompressible viscoelastic fluid. Figures 3(a), 3(c), and 3(d) display the unstable (red) regions of the parameter space and the passive (blue) regions, where the thermodynamics constraint (6) is satisfied. These two regions are disjoint, as expected from thermodynamics. Note that the three-dimensional view of the parameter space $(\nu_o, \gamma_s\eta_s, \gamma_s\eta_s)$ of Fig. 3(d) shows the symmetry $(\nu_o, \gamma_o) \to (-\nu_o, -\gamma_o)$ of the system.

As intuition would suggest, the friction γ_s, which characterizes the elastic stress relaxation, has a stabilizing role, and increasing it always leads to more stable systems. On the other hand, the odd coupling ν_o is destabilizing the system as its magnitude is increased (provided its sign is kept constant). The odd elastic relaxation term γ_o has a more subtle effect and may have a destabilizing or stabilizing influence [see Fig. 3(a)].

Figure 3(b) highlights the consequences of the odd active coefficients on the time-dependent (drag) response $M_\parallel(t)$ experienced by the particle along its velocity. In the linearly stable regions [points A and B in Fig. 3(a)], the drag decays to 0, indicating that the initial perturbation is eventually damped by viscous friction. On the other hand, the parallel response corresponding to parameters in the active unstable region [point C in Fig. 3(a)] increases with time, indicating that the probe motion is accelerated by the active fluid surrounding it. This acceleration must eventually be compensated by nonlinearities that we have not considered in the present analysis.

Broken Onsager symmetry. We now continue the discussion in the case of an incompressible fluid with broken Onsager symmetry, that is, $\boldsymbol{\nu}' \neq \boldsymbol{\nu}$. We define $\nu'_{s,o} = \tilde{\nu}_{s,o} + e_{s,o}$ and $\nu_{s,o} = \tilde{\nu}_{s,o} - e_{s,o}$, such that the Onsager symmetry is recovered for $e_{s,o} = 0$. Breaking Onsager symmetry modifies the conditions for stability, although these new conditions take a form similar to those given in Eq. (21). They read

$$e_o^2 - e_s^2 + 4\gamma_s\eta_s - \tilde{\nu}_o^2 + \tilde{\nu}_s^2 > 0, \qquad (22a)$$

$$2\eta_s\gamma_o^2 + 2\gamma_o\tilde{\nu}_o\tilde{\nu}_s + \gamma_s\big(2\gamma_s\eta_s - \tilde{\nu}_o^2 + \tilde{\nu}_s^2\big) + \gamma_- > 0, \qquad (22b)$$

where $\gamma_\pm = \gamma_s(e_o^2 - e_s^2) \pm 2\gamma_o e_s e_o$, and

$$\Delta < 0 \text{ or } \begin{cases} \Delta \geqslant 0 \quad \text{and} \\ \gamma_s\big(\tilde{\nu}_s^2 - \tilde{\nu}_o^2\big) - 2\gamma_o\tilde{\nu}_o\tilde{\nu}_s + 8\eta_s\gamma_s^2 + \gamma_+ < 0, \end{cases} \qquad (22c)$$

where we have defined $\Delta = b_1^2 - 4b_0 b_2$ with $b_1 = G_s^2[\gamma_s(8\gamma_s\eta_s - \tilde{\nu}_o^2 + \tilde{\nu}_s^2) - 2\gamma_o\tilde{\nu}_o\tilde{\nu}_s + \gamma_+]/(\tau_0\eta_s)$, $b_2 = G_s(e_o^2 - e_s^2 + 4\gamma_s\eta_s - \tilde{\nu}_o^2 + \tilde{\nu}_s^2)/(\tau_0^2\eta_s)$. Importantly, note that e_o cannot destabilize the system. This is expected, as this coefficient enters antisymmetrically in the constitutive equations, which causes its contribution to the entropy production to vanish. In fact, taking $e_s = 0$ in Eq. (22) shows that the constraints are more easily satisfied for $e_o \neq 0$, and e_o even has a stabilizing effect.

On the other hand, e_s does add to the dissipation rate, and therefore a nonvanishing e_s can drive the system into an unstable regime, even if the symmetric equivalent of thermodynamic constraint $2\eta_s\gamma_s \geqslant \tilde{\nu}_o^2$ is satisfied. If $e_s \neq 0$ and $\gamma_o \neq 0$, the odd deviation from Onsager symmetry e_o can also
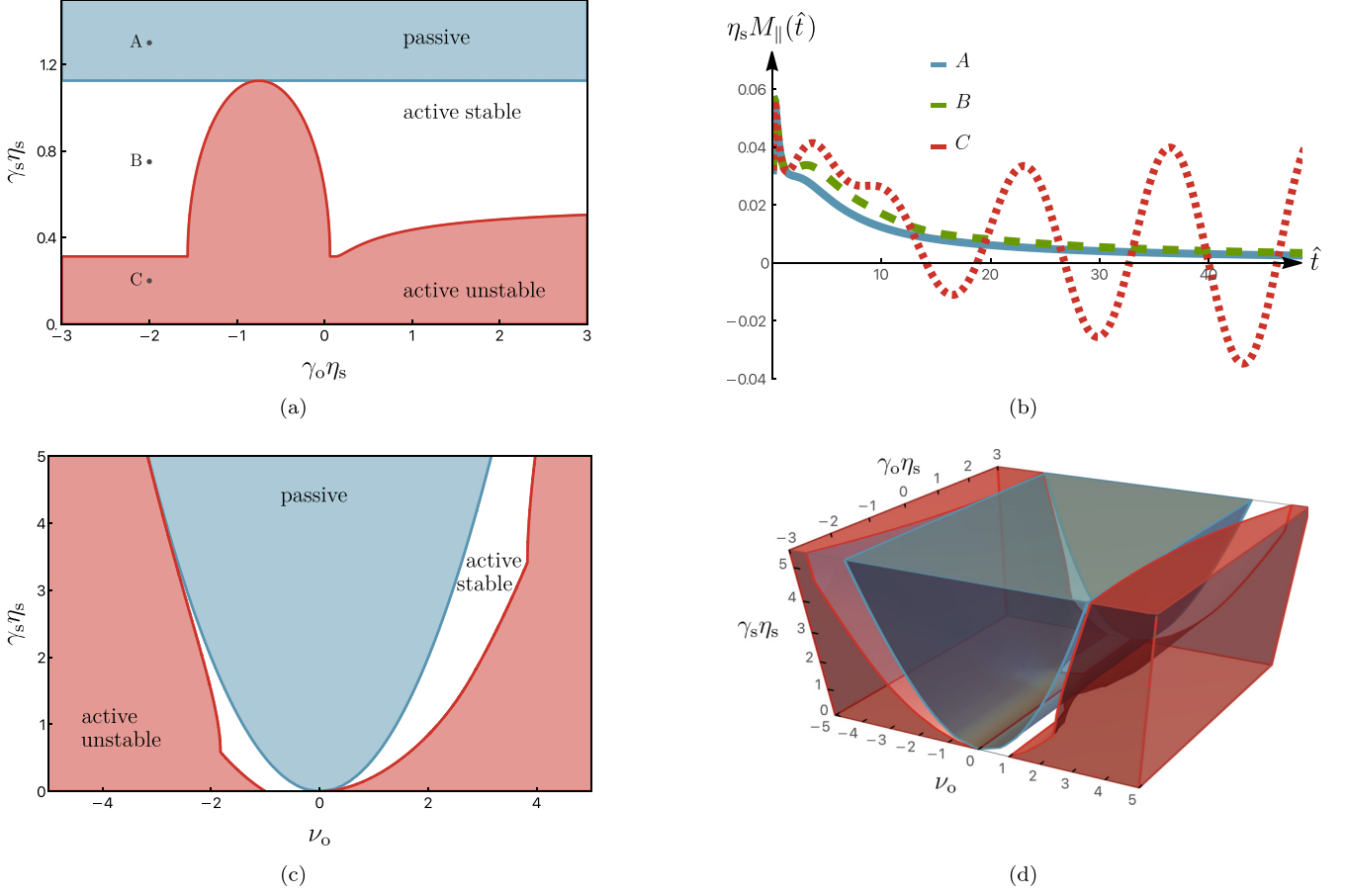
FIG. 3. Stability of a probe in an odd viscoelastic medium. (a,c) Stable (white and blue) and linearly unstable (red) regions in the parameter space $(\gamma_o \eta_s, \gamma_s \eta_s)$ in panel (a) and $(\nu_o, \gamma_s \eta_s)$ in panel (c). The passive (blue) region indicates where the passivity constraint (6) is satisfied. (b) Drag response $\eta_s M_\parallel$ as a function of the dimensionless time $\hat{t} = t/\tau_0$ with $\tau_0 = a^2 \rho_0 / \eta_s$ for the points A, B, C in the parameter space indicated in panel (a). (d) Linearly unstable (red) and passive (blue) regions in the three-dimensional parameter space $(\nu_o, \gamma_o \eta_s, \gamma_s \eta_s)$. Importantly, the transformation $(\nu_o, \gamma_o) \to (-\nu_o, -\gamma_o)$ is a symmetry of the system. Parameters used are as follows: for all panels, $\nu_s = 1$. (a) $\nu_o = 1.5$. (b) A, B, C: $\nu_o = 1.5$, $\gamma_o \eta_s = -2$, $G_s \tau_0 / \eta_s = 0.25$, and A: $\gamma_s \eta_s = 1.3$, B: $\gamma_s \eta_s = 0.75$, C: $\gamma_s \eta_s = 0.2$. (c) $\gamma_o \eta_s = 2$.

play a role in destabilizing the system through the term $\gamma_o e_s e_o$ entering Eq. (22). These results show the complex interplay between oddity and the breaking of Onsager symmetry in determining the stability of a probe.

IV. DRAG AND LIFT RESPONSE

A. Drag response for an incompressible fluid

In this section, we consider the response along the velocity direction [drag, $M_\parallel(s)$] and perpendicular to it [lift, $M_\perp(s)$], making the decomposition

$$\mathbb{M}_{ij}(s) = M_\parallel(s)\delta_{ij} - M_\perp(s)\varepsilon_{ij}. \qquad (23)$$

For simplicity, we enforce Onsager symmetry in this section and take $\boldsymbol{v}' = \boldsymbol{v}$. We first consider the incompressible limit, so that $M_\perp^{\mathrm{inc}}(s) = 0$, whereas the drag response coefficient reads

$$M_\parallel^{\mathrm{inc}}(s) = \frac{1}{4\pi A_s(s)} K_0\left(\sqrt{\frac{s\tau_0}{A_s(s)/\eta_s}} \right), \qquad (24)$$

with $\tau_0 = \rho_0 a^2 / \eta_s$, and $K_0(z)$ is the zeroth modified Bessel function of the second kind. The corresponding drag response

in time domain can be obtained numerically (see Appendix F for details), and the results are displayed in Fig. 4.

In Figs. 4(a) and 4(b), we first explore the role of the odd elastic coefficient ν_o and of the odd elastic strain relaxation rate γ_o. For a vanishing odd elastic strain relaxation rate γ_o [Fig. 4(a)], the drag response does not display oscillations, while a nonvanishing γ_o [Fig. 4(b)] leads to a long-lived oscillatory behavior, despite strain relaxation due to plasticity. This is a unique property that can signal odd viscoelasticity in experiments. Furthermore, we note that the amplitude of these oscillations is strongly amplified by the odd elasticity coefficient ν_o. This finding highlights again the nontrivial interplay between the different odd coefficients, which was already observed in Sec. III B for the stability constraints. It shows that increasing γ_o and ν_o eventually induces instabilities. Specifically, the dotted red line in Fig. 4(a) (corresponding to $\nu_o \geqslant \gamma_s^2 + \nu_s^2$) corresponds to a diverging trajectory. Such a nonconverging drag response should be regularized by nonlinear corrections.

In Figs. 4(c) and 4(d), we compute the drag response for a varied γ_o for $\nu_o = 0$ and 1, respectively. We find that an increasing γ_o leads to an increasing oscillation frequency. In Fig. 4(d), the choice of ν_o makes the viscoelastic fluid active,
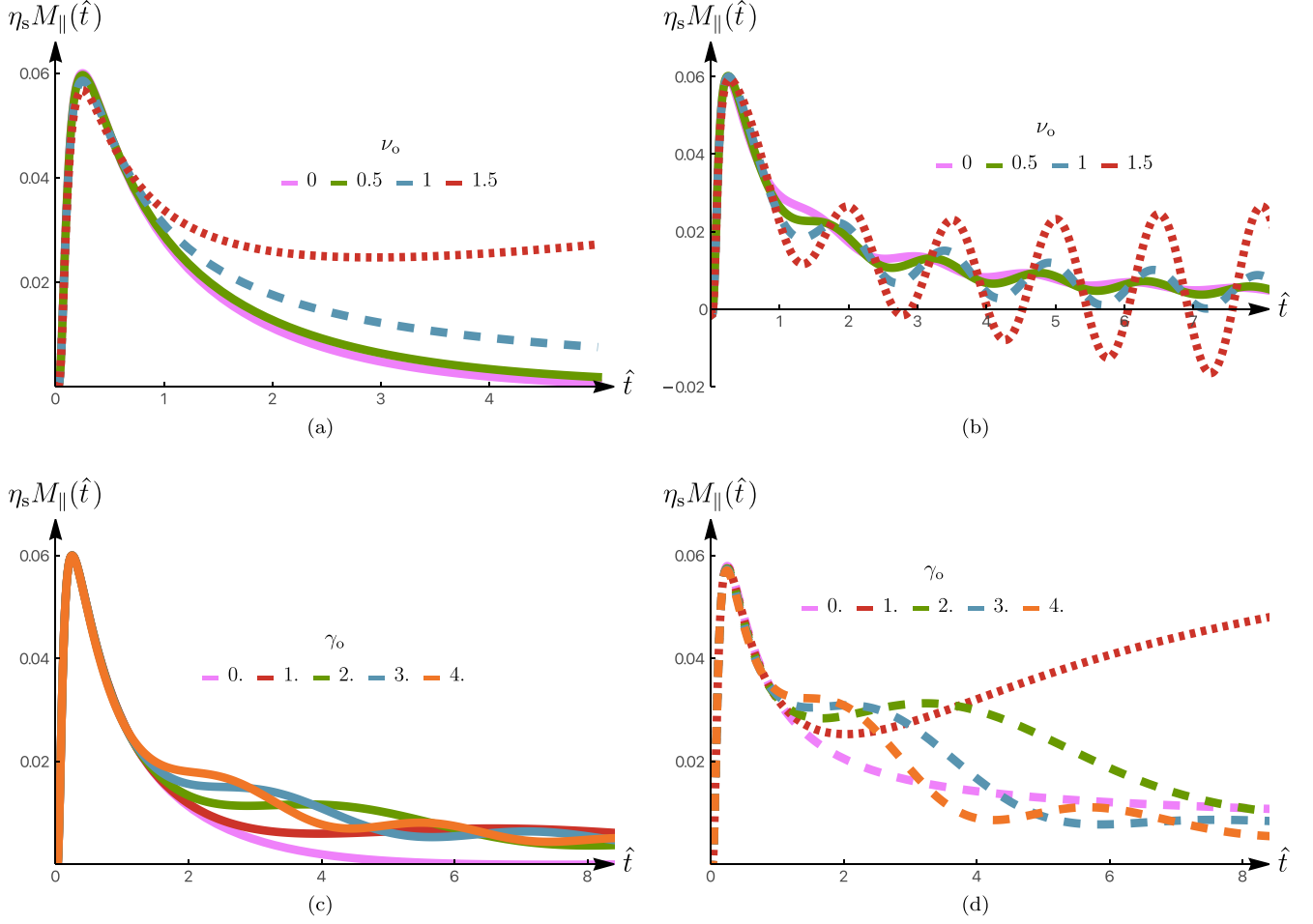
FIG. 4. Drag response $\eta_s M_\parallel$ of an odd incompressible viscoelastic fluid as a function of the dimensionless time $\hat{t} = t/\tau_0$ with $\tau_0 = a^2\rho_0/\eta_s$. (a) In the absence of an odd elastic stress relaxation ($\gamma_o = 0$) and for different values of ν_o. (b) In the presence of an odd elastic stress relaxation ($\gamma_o \eta_s = 8$) and for different values of ν_o. (c) Drag response for a varied odd elastic stress relaxation γ_o and a vanishing ν_o. (d) Drag response for a varied odd elastic stress relaxation γ_o and $\nu_o = -1.2$. In all panels, the solid lines indicate passive fluids for which Eq. (6) is satisfied, while dashed lines are used for active fluids. The red dotted lines are unstable active drag responses for which Eq. (21) is violated. Such responses diverge at long time, and nonlinear mechanisms should be included to obtain the corresponding large-time behavior. Other parameters are $\nu_s = 1$, $\gamma_s \eta_s = 0.3$, $G_s \tau_0/\eta_s = 0.25$.

and it was shown in Sec. III B that this may induce instabilities for the motion of the probe particle. This is the case for the dotted red line, which violates the stability constraint of Eq. (21b).

B. Drag and lift response for a compressible fluid

Compressibility is a necessary condition for observing lift forces [18,39], a signature of odd fluids. In this section, we thus discuss how a finite compressibility of the fluid can be considered within our framework. Although exploring systematically the role of finite compressibility for the response of a probe in an odd viscoelastic medium is beyond the scope of this paper, we illustrate here a few important features of finite compressibility.

To relax the incompressibility constraint while continuing analytic computations, we consider a weak oddity approximation, i.e., we consider η_o, γ_o, and ν_o small compared to their shear and bulk counterparts. We introduce ε_o, the corresponding small parameter (for instance, $\varepsilon_o = \eta_o/\eta_s$). We

discuss here the first nonvanishing correction, although the series expansion can be continued to higher orders. Starting from Eq. (15), we obtain the response coefficients that were defined in Eq. (23):

$$M_\parallel(s) = M_\parallel^{\mathrm{inc}}(s) + \frac{\Theta(s)K_0(\sqrt{\tau_0 s \Theta(s)})}{4\pi\eta_s} + O(\varepsilon_o^2),$$

(25a)

$$M_\perp(s) = \frac{\tau_0 s A_o(s)/\eta_s}{\hat{\psi}^{-1} + \tau_0 s A_b(s)/\eta_s}\left[2M_\parallel^{\mathrm{inc}}(s) - \frac{\Theta(s)K_0(\sqrt{\tau_0 s \Theta(s)})}{2\pi\eta_s}\right] + O(\varepsilon_o^2),$$

(25b)

where we have defined the dimensionless compressibility $\hat{\psi} = \psi\eta_s^2/(a\rho_0)^2$ and

$$\Theta(s) = \frac{\tau_0 s}{\hat{\psi}^{-1} + \tau_0 s[A_b(s) + A_s(s)]/\eta_s}.$$
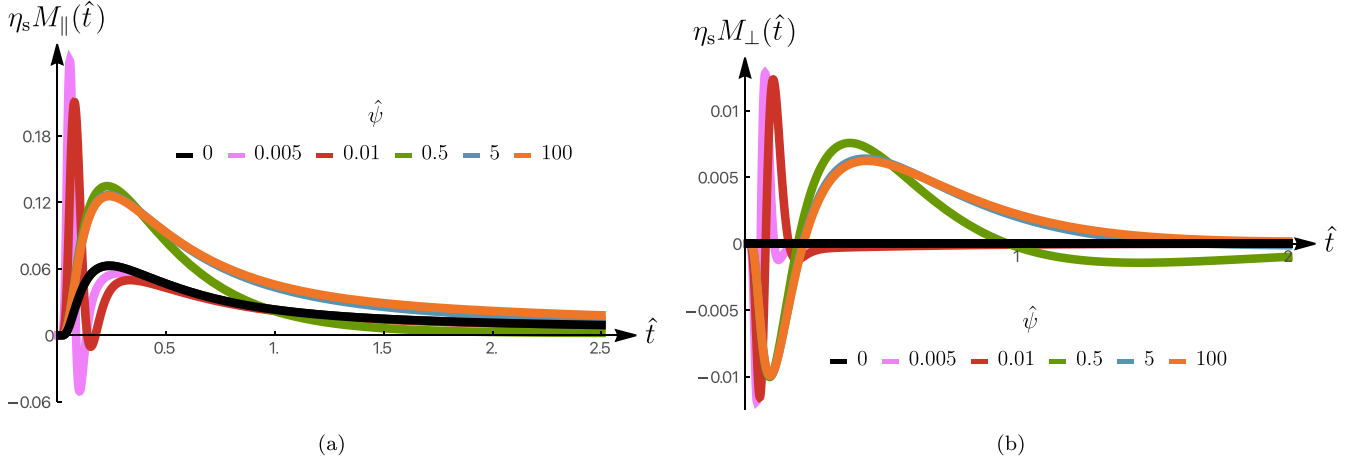
(25c)

FIG. 5. Drag and lift responses of an odd compressible viscoelastic fluid induced as a function of the dimensionless time $\hat{t} = t/\tau_0$ with $\tau_0 = a^2 \rho_0 / \eta_s$. (a) Drag response $\eta_s M_\parallel$ for different values of the dimensionless inverse compressibility $\hat{\psi} = \psi \eta_s^2 / (a \rho_0)^2$. (b) Lift response $\eta_s M_\perp$ for different values of the dimensionless inverse compressibility $\hat{\psi}$. Other parameters are $\nu_s = \nu_b = 1$, $\gamma_s \eta_s = 1$, $G_s \tau_0 / \eta_s = 1$, $\eta_b / \eta_s = 0$, $\gamma_b \eta_s = 0$, $G_b \tau_0 / \eta_s = 0$, $\eta_o / \eta_s = 0.1$, $\gamma_o \eta_s = 0.1$, $\nu_o = 0$.

As expected, the lift response vanishes in the incompressible limit $\hat{\psi} \to 0$. Note also the absence of odd corrections to the drag response [Eq. (25a)] at first order.

Figure 5 displays the drag and lift responses for different values of $\hat{\psi}$, illustrating the role of a finite compressibility. Increasing the compressibility $\hat{\psi}$ spreads out the response in time both for the drag and lift coefficients. For small values of the compressibility, we observe a short-time response, eventually converging to the incompressible limit [black line, Fig. 5(a)]. The lift response, which is a hallmark of odd systems and thus vanishes in the absence of the odd coefficients, is shown in Fig. 5(b). Note the rapid sign change of the lift coefficient, which becomes more pronounced and symmetrical as the compressibility $\hat{\psi}$ is decreased, leading eventually to a vanishing lift response in the incompressible limit $\hat{\psi} \to 0$.

V. DISCUSSION

In this work, we considered the stability of two-dimensional odd viscoelastic fluids by looking at the motion of probe particles that experience an instantaneous push at $t = 0$. We considered contributions to the constitutive equation that are allowed for passive systems (as found in Ref. [3]), as well as active terms that rely on fuel consumption at a microscopic level. Such active terms modify the passive picture by breaking the two hallmarks of passive hydrodynamics: Onsager-symmetry and positive-definiteness of the Onsager matrices. To characterize the effect of activity, we first discussed the stability condition of a probe in a generic, compressible odd viscoelastic fluid before focusing on the incompressible limit, where the discussion is simpler while the essential ingredients are kept. Importantly, although the lift force vanishes in this limit [17], odd viscoelastic effects manifest themselves spectacularly as they can destabilize the probe motion. We find that passive odd viscoelastic fluids, where viscoelastic coefficients are constrained by the Second Law of Thermodynamics, are always linearly stable. We find the converse statement that active odd viscoelastic fluids are always unstable not to be true. Specifically, we find that there

is an intermediate region where the motion of probe particles is stable, despite the system being active and constantly consuming fuel. In this intermediate regime, there is a nontrivial interplay between the odd elasticity coefficient ν_o and odd plasticity γ_o, which is graphically displayed in Fig. 3. This interplay is even more surprising considering that odd plasticity is a nondissipative phenomenon and therefore plays no role in determining the passivity of an odd viscoelastic fluid [3]. Similarly, the nondissipative shear elastic coefficient ν_s is involved in stability constraints despite being nondissipative.

The stability of viscoelastic models was considered in previous works by looking at the stability of perturbative modes. In Ref. [3], a small wave-vector analysis yielded a constraint identical to Eq. (21b), which is one of the three constraints obtained in this work for stable probe particle motion that are given in Eq. (21). In Ref. [25], odd viscoelastic materials were studied in the context of the formation of spatial-temporal patterns, whose presence indicates instability. The authors performed a numerical analysis of the perturbative modes to determine their stability for a range of wave vectors. The numerical findings of Ref. [25], showing that odd elasticity can destabilize the viscoelastic material, whereas shear elasticity, plasticity, and viscosity tend to stabilize the viscoelastic material, qualitatively agree with the analytic constraints derived in the present work. Such a qualitative finding is also consistent with the analytically derived stability constraint of Eq. (21b) found in Ref. [3].

In this work, we furthermore considered the effect of several odd viscoelastic coefficients on probe particle motion. The obtained results provide a viscoelastic extension of Ref. [18] for the incompressible case and of Refs. [39,40] for the compressible case, which considered lift and drag force for an odd viscous fluid. When generalizing to viscoelastic fluids, one must consider inhomogeneities in time to see qualitatively different effects, as at vanishing frequencies only viscous effects remain. For this reason, we only considered the motion of a probe particle after a push at $t = 0$. A computational advantage of doing so is that there is no problem arising from the Stokes paradox [51], which for the steady case was

resolved in Refs. [39,40] by regularizing the integral with momentum relaxation coming from the three-dimensional bulk. We first considered the incompressible limit, which is a limit that is decoupled from passivity constraints and therefore a useful limit for considering active destabilizing effects. One key qualitative feature that we find is that the relaxing velocity becomes oscillatory for a nonzero odd plasticity coefficient γ_o and that the amplitude of this oscillation is amplified by the odd elasticity coefficient ν_o. This again highlights the nontrivial interplay between these two odd viscoelastic coefficients, and it is illustrated in Fig. 4. We also discussed the role of compressibility in the response of the probe. In this case, we showed that the odd lift force, transverse to the direction of motion of the probe particle, that exists for viscous odd fluids, becomes time-dependent in viscoelastic systems. We discussed this case focusing on a small oddity limit, where analytical results can be obtained, and the results are displayed in Fig. 5. In the compressible regime, probes placed in a linearly unstable odd viscoelastic fluid are likely to perform limit cycles in the plane. Exploring these limit cycles, and more generally the probe motion in the linearly unstable regime, is an interesting aspect that requires introducing nonlinear terms whose symmetry and time dependence need to be discussed. We leave this work for future publications.

Lastly, chiral biological systems such as cell assemblies or tissues are good candidates for displaying simultaneously odd, active, and viscoelastic behaviors. In this context, a layer of such cells is likely to exchange momentum with the three-dimensional bulk (for instance, an extracellular matrix in the case of an epithelial tissue, or seawater in the case of starfish oocytes [11]). In addition, cell number is usually not conserved in such systems since cell divisions, deaths, or extrusions can occur. Although we have not considered finite momentum or density relaxation processes in this paper, taking them into account would be straightforward [52,53] in our formalism. The effects of such terms have been discussed for purely viscous odd fluids in Ref. [39].

APPENDIX A: CONSTITUTIVE EQUATIONS FOR ACTIVE ODD MATERIALS

In this Appendix, we will derive the most general constitutive equations for the conserved currents by constraining entries using the Onsager relations and the Second Law of Thermodynamics. In Appendix A 1, we first consider the passive case, following to a large extent the steps performed in Ref. [45]. This analysis will yield a result that coincides with Ref. [3], where a general model for passive odd viscoelasticity was constructed. Then we consider the active case in Appendix A 2. Here, as in Ref. [46], we add fuel consumption, which allows for a much broader class of nonequilibrium corrections, for which we consider the effect of some of them on the motion of beads in the main text.

1. Passive chiral viscoelastic fluid

To hydrodynamically describe a viscoelastic fluid, we first formulate the conservation laws in the absence of external forces and torques. First, there is conservation of mass density ρ and momentum g_i,

$$\partial_t \rho + \partial_i(\rho v_i) = 0, \tag{A1a}$$

$$\partial_t g_i - \partial_j \sigma_{ij}^{\text{tot}} = 0, \tag{A1b}$$

where σ_{ij}^{tot} is the total stress and v_i is the fluid velocity. Momentum is related to fluid velocity as $g_i = \rho v_i$. In addition, we have conservation of angular momentum, given by

$$\partial_t l_{ij} + \partial_k M_{ijk} = -2\sigma_{[ij]}^{\text{tot}}, \tag{A1c}$$

where l_{ij} is the density of intrinsic angular momentum, M_{ijk} is the angular momentum flux and where $\sigma_{[ij]}^{\text{tot}} = (\sigma_{ij}^{\text{tot}} - \sigma_{ji}^{\text{tot}})/2$ denotes the antisymmetric part of the total stress. Another property that is important for describing the state of viscoelastic fluids is the tensor u_{ij}. In the elastic limit, u_{ij} is the elastic strain, however for general viscoelastic fluids u_{ij} can undergo relaxation through plastic deformations [54,55]. To study the evolution of u_{ij} and the behavior the viscoelastic fluid in general, we start by formulating a local free energy [45,46]:

$$\mathcal{F} = \int \left(\frac{1}{2}\rho v^2 + f(u_{ij}) \right) dV, \tag{A2}$$

where $f(u_{ij})$ is the local free-energy density, which depends on u_{ij}. The tensor u_{ij} is conjugate to the local elastic stress σ_{ij}^{el}, such that $\sigma_{ij}^{\text{el}} = \partial f/\partial u_{ij}$. For an isotropic solid, the local free energy density at leading order in strain is given by

$$f(u_{ij}) = f_0 + G_s(\tilde{u}_{ij})^2 + \frac{1}{2}G_b(u_{jj})^2. \tag{A3}$$

To derive the constitutive equations for the viscoelastic fluid using the standard hydrodynamic approach, we decompose our stress into

$$\sigma_{ij}^{\text{tot}} = -\rho v_i v_j - P\delta_{ij} + \sigma_{ij}^{\text{s}} + \sigma_{ij}^{\text{a}}, \tag{A4}$$

where σ_{ij}^{s} is the deviatoric stress, which is symmetric, and σ_{ij}^{a} is the antisymmetric contribution to the stress. The pressure P is obtained with the Euler relation

$$P = -f + \mu n, \tag{A5}$$

with μ being the chemical potential, and where the density n is given by $n = \rho/m$. If one considers the change of time of F, one finds upon plugging in the conservation laws of Eq. (A1) that the entropy production rate Θ is given by [45,46]

$$T\Theta = \sigma_{ij}^{\text{s}} v_{ij} - \frac{Du_{ij}}{Dt}\sigma_{ij}^{\text{el}} + \frac{1}{2}\partial_k \omega_{ij} M_{ijk}, \tag{A6}$$

where we introduced the rotation $\omega_{ij} = \frac{1}{2}(\partial_i v_j - \partial_j v_i)$ as well as the corotational derivative, which for a general two-tensor

a_{ij} is given by

$$\frac{\mathrm{D}a_{ij}}{\mathrm{D}t} = \partial_t a_{ij} + v_k \partial_k a_{ij} + \omega_{ik} a_{kj} + \omega_{jk} a_{ik}. \quad \text{(A7)}$$

The presence of the corotational derivative in Eq. (A6) follows from the requirement that the free energy is invariant under rotations [45]. To have a corotational derivative on the strain field requires the antisymmetric stress to take the form $\sigma_{ij}^{\mathrm{a}} = u_{ik}\sigma_{kj}^{\mathrm{el}} - u_{jk}\sigma_{ki}^{\mathrm{el}}$. Because of the conservation of angular momentum given by Eq. (A1c), there is no contribution coming from the antisymmetric stress in the entropy production rate of Eq. (A6) [56]. Instead, there is only a contribution from the deviatoric angular momentum flux M_{ijk}, which will give contributions to the equations of motion that are two orders higher in gradients, and these contributions will therefore be omitted. Note that because odd viscoelastic fluids are often introduced by chiral agents that draw arbitrary amounts of angular momentum from the environment, the conservation of angular momentum tends not to hold. In the absence of angular momentum conservation, there are ways in which the antisymmetric stress can get hydrodynamic corrections. However, we will omit these antisymmetric contributions for simplicity by upholding angular momentum conservation. Having the entropy production rate of Eq. (A6) at our disposal, we are now ready to construct the Onsager matrix, which contains the most general entries in the deviatoric currents. An important difference compared to the isotropic achiral viscoelastic fluids in two dimensions is that, in addition to the identity, the fully antisymmetric two-dimensional Levi-Civita tensor ε_{ij} can be used to construct entries in the constitutive equations. As we will discuss below, these tensors can feature components that are odd under the exchange of indices. This can give rise, for example, to odd viscosity [6,57–59]. Such terms signal parity-breaking, and for passive two-dimensional systems one often finds that this breaking of parity is accompanied by a breaking of time-reversal symmetry, as is the case, for example, for parity-breaking induced by a background magnetic field. We therefore uphold symmetry under the simultaneous transformation of parity and time-reversal when deriving the passive constitutive equations, which modify the Onsager relations. The details of this are provided in Appendix C. From the expression of entropy production (A6) and the Onsager relations, we obtain the following constitutive relations:

$$\sigma_{ij}^{\mathrm{s}} = 2\eta_{\mathrm{s}}^{\mathrm{p}}\tilde{v}_{ij} + \eta_{\mathrm{b}}^{\mathrm{p}}v_{kk}\delta_{ij} + 2\eta_{\mathrm{o}}^{\mathrm{p}}v_{ij}^{\mathrm{o}} + \nu_{\mathrm{s}}^{\mathrm{p}}\sigma_{ij}^{\mathrm{el}}$$
$$+ \frac{1}{2}\nu_{\mathrm{b}}^{\mathrm{p}}\sigma_{kk}^{\mathrm{el}}\delta_{ij} + \nu_{\mathrm{o}}^{\mathrm{p}}(\sigma^{\mathrm{el}})_{ij}^{\mathrm{o}}, \quad \text{(A8a)}$$

$$\frac{\mathrm{D}u_{ij}}{\mathrm{D}t} = -\gamma_{\mathrm{s}}^{\mathrm{p}}\tilde{\sigma}_{ij}^{\mathrm{el}} - \frac{1}{2}\gamma_{\mathrm{b}}^{\mathrm{p}}\sigma_{kk}^{\mathrm{el}}\delta_{ij} - \gamma_{\mathrm{o}}^{\mathrm{p}}(\sigma^{\mathrm{el}})_{ij}^{\mathrm{o}} + \nu_{\mathrm{s}}^{\mathrm{p}}v_{ij}$$
$$+ \frac{1}{2}\nu_{\mathrm{s}}^{\mathrm{p}}v_{kk}\delta_{ij} + \nu_{\mathrm{o}}^{\mathrm{p}}v_{ij}^{\mathrm{o}}. \quad \text{(A8b)}$$

What we see in Eq. (A8) are the shear, bulk, and odd viscosity given by the η-terms, as well as γ-terms representing shear and bulk plasticity, as well as a coefficient that could be called "odd plasticity." This odd plasticity was first considered in Ref. [60]. Then, there are ν-terms that are nonequilibrium corrections representing shear, bulk, and odd elasticity, the latter of which was first considered as an active term

in Ref. [23]. Using the compact notation described in Appendix B, Eq. (A8) can be rewritten as

$$\underline{\underline{\sigma}}^{\mathrm{s}} = \boldsymbol{\nu}^{\mathrm{p}} : \underline{\underline{\sigma}}^{\mathrm{el}} + 2\boldsymbol{\eta}^{\mathrm{p}} : \underline{v}, \quad \text{(A9a)}$$

$$\frac{\mathrm{D}\underline{\underline{u}}}{\mathrm{D}t} = -\boldsymbol{\gamma}^{\mathrm{p}} : \underline{\underline{\sigma}}^{\mathrm{el}} + \boldsymbol{\nu}^{\mathrm{p}} : \underline{v}. \quad \text{(A9b)}$$

To see the dissipative properties of the entries in the constitutive equations of Eq. (A9), we plug Eq. (A8) back into Eq. (A6), which yields

$$T\Theta = \mathrm{Tr}\big[2\eta_{\mathrm{s}}^{\mathrm{p}}\underline{\tilde{v}} \cdot \underline{\tilde{v}} + 2\nu_{\mathrm{o}}^{\mathrm{p}}(\underline{\tilde{\sigma}}^{\mathrm{el}} \cdot \underline{\varepsilon} \cdot \underline{\tilde{v}})$$
$$+ \gamma_{\mathrm{s}}^{\mathrm{p}}\underline{\tilde{\sigma}}^{\mathrm{el}} \cdot \underline{\tilde{\sigma}}^{\mathrm{el}}\big] + 2\eta_{\mathrm{b}}^{\mathrm{p}}\mathrm{Tr}[v]^2 + \gamma_{\mathrm{b}}^{\mathrm{p}}\mathrm{Tr}[v]^2. \quad \text{(A10)}$$

Requiring the first term on the right-hand side of Eq. (A10) to be non-negative is equivalent to requiring that the matrix

$$\begin{pmatrix} 2\eta_{\mathrm{s}}^{\mathrm{p}}\underline{\underline{\mathbb{1}}} & -\nu_{\mathrm{o}}^{\mathrm{p}}\underline{\varepsilon} \\ \nu_{\mathrm{o}}^{\mathrm{p}}\underline{\varepsilon} & \gamma_{\mathrm{s}}^{\mathrm{p}}\underline{\underline{\mathbb{1}}} \end{pmatrix} \quad \text{(A11)}$$

is semidefinite-positive, which is satisfied if all its eigenvalues have a non-negative real part. As was found in Ref. [3], this condition is guaranteed if, in addition to $\eta_{\mathrm{s}}^{\mathrm{p}}, \gamma_{\mathrm{s}}^{\mathrm{p}}, \eta_{\mathrm{b}}^{\mathrm{p}}, \gamma_{\mathrm{b}}^{\mathrm{p}} \geqslant 0$, we have

$$2\eta_{\mathrm{s}}^{\mathrm{p}}\gamma_{\mathrm{s}}^{\mathrm{p}} \geqslant (\nu_{\mathrm{o}}^{\mathrm{p}})^2, \quad \text{(A12)}$$

which is the thermodynamic constraint given in Eq. (4).

2. Active chiral viscoelastic fluid

The passive model we have introduced above can be generalized by considering activity induced by microscopic fuel consumption of microscopic agents [46]. The rate of fuel consumption can be represented by $\Delta\mu$, which is the chemical potential difference of a chemical reaction, multiplied by a scalar reaction rate r. Because of this fuel consumption, the entropy production rate of Eq. (A6) is generalized to

$$T\Theta = \sigma_{ij}^{\mathrm{s}}v_{ij} - \frac{\mathrm{D}u_{ij}}{\mathrm{D}t}\sigma_{ij}^{\mathrm{el}} + \frac{1}{2}\partial_k\omega_{ij}M_{ijk} + r\Delta\mu. \quad \text{(A13)}$$

This new contribution opens up a wide range of new possible entries in the constitutive equations, which are given by

$$\underline{\underline{\sigma}}^{\mathrm{s}} = \boldsymbol{\nu}^{\mathrm{p}} : \underline{\underline{\sigma}}^{\mathrm{el}} + 2\boldsymbol{\eta}^{\mathrm{p}} : \underline{v} + \Delta\mu(\boldsymbol{\zeta}^{(1)} : \underline{\underline{\sigma}}^{\mathrm{el}} + 2\boldsymbol{\zeta}^{(2)} : \underline{v}),$$
$$\text{(A14a)}$$

$$\frac{\mathrm{D}\underline{\underline{u}}}{\mathrm{D}t} = -\boldsymbol{\gamma}^{\mathrm{p}} : \underline{\underline{\sigma}}^{\mathrm{el}} + \boldsymbol{\nu}^{\mathrm{p}} : \underline{v} + \Delta\mu(-\boldsymbol{\zeta}^{(3)} : \underline{\underline{\sigma}}^{\mathrm{el}} + \boldsymbol{\zeta}^{(4)} : \underline{v}).$$
$$\text{(A14b)}$$

The active terms ($\propto \Delta\mu$) can be absorbed into a redefinition of the parameters so that constitutive equations read

$$\underline{\underline{\sigma}}^{\mathrm{s}} = \boldsymbol{\nu} : \underline{\underline{\sigma}}^{\mathrm{el}} + 2\boldsymbol{\eta} : \underline{v}, \quad \text{(A15a)}$$

$$\frac{\mathrm{D}\underline{\underline{u}}}{\mathrm{D}t} = -\boldsymbol{\gamma} : \underline{\underline{\sigma}}^{\mathrm{el}} + \boldsymbol{\nu}' : \underline{v}, \quad \text{(A15b)}$$

which is Eq. (5) in the main text. The new parameters are related to the passive ones of Eq. (A14) by $\boldsymbol{\eta} = \boldsymbol{\eta}^{\mathrm{p}} + \Delta\mu\boldsymbol{\zeta}^{(2)}$, $\boldsymbol{\gamma} = \boldsymbol{\gamma}^{\mathrm{p}} + \Delta\mu\boldsymbol{\zeta}^{(3)}$, $\boldsymbol{\nu} = \boldsymbol{\nu}^{\mathrm{p}} + \Delta\mu\boldsymbol{\zeta}^{(1)}$, and $\boldsymbol{\nu}' = \boldsymbol{\nu}^{\mathrm{p}} + \Delta\mu\boldsymbol{\zeta}^{(4)}$. Note that $\Delta\mu$, as can be seen in Eq. (A13), is a thermodynamic force [46] corresponding to the flux r. Because $\Delta\mu$ is a thermodynamic force, it should be a small correction with

respect to the local equilibrium. This means that the $\Delta\mu\underline{\underline{\sigma}}^{\text{el}}$- and $\Delta\mu\underline{v}$-terms are second order, and one would therefore naively think that these terms should be neglected. However, these second-order terms play an important qualitative role as the effective coefficients appearing in $\boldsymbol{\eta}, \boldsymbol{\gamma}, \boldsymbol{\nu}, \boldsymbol{\nu}'$ are not bound by the passivity constraint (A12). In particular, this allows for the presence of active odd elasticity.

To make sure that the second law constraint $\Theta \geqslant 0$ in Eq. (A13) as well as the Onsager relations described in Appendix C are satisfied, we require the corresponding reaction rate to be

$$
\begin{aligned}
r = \Lambda\Delta\mu + \text{Tr}[&-\underline{\underline{\sigma}}^{\text{el}} : \boldsymbol{\zeta}^{(1)} : \underline{v} + 2\underline{v} : \boldsymbol{\zeta}^{(2)} : \underline{v} \\
&+ \underline{\underline{\sigma}}^{\text{el}} : \boldsymbol{\zeta}^{(3)} : \underline{\underline{\sigma}}^{\text{el}} + \underline{v} : \boldsymbol{\zeta}^{(4)} : \underline{\underline{\sigma}}^{\text{el}}].
\end{aligned}
\tag{A16}
$$

APPENDIX B: COMPACT TENSOR NOTATION AND ODD ISOTROPIC RANK-4 TENSOR ALGEBRA

In this Appendix, we describe the notation used for describing tensors and their contractions. First, we describe vectors and two-tensors with a single and a double underline, i.e.,

$$
V_i \to \underline{V}, \quad T_{ij} \to \underline{\underline{T}}.
\tag{B1}
$$

We define the components of an odd isotropic rank-4 tensor $\boldsymbol{B}$ in the following way:

$$
\begin{aligned}
B_{ijkl} = \frac{B_{\text{s}}}{2}(\delta_{ik}\delta_{jl} + \delta_{il}\delta_{jk} - \delta_{ij}\delta_{kl}) + \frac{B_{\text{b}}}{2}\delta_{ij}\delta_{kl} \\
+ \frac{B_{\text{o}}}{4}(\delta_{ik}\varepsilon_{jl} + \delta_{il}\varepsilon_{jk} + \delta_{jk}\varepsilon_{il} + \delta_{jl}\varepsilon_{ik}).
\end{aligned}
\tag{B2}
$$

These tensors are symmetric with respect to their first two and last two indices, such that $B_{ijkl} = B_{jikl}$ and $B_{ijkl} = B_{ijlk}$. The contraction of an odd isotropic rank-4 tensor $\boldsymbol{B}$ with an arbitrary rank-2 tensor $\underline{\underline{b}}$ reads

$$
(\boldsymbol{B} : \underline{\underline{b}})_{ij} = B_{ijkl}b_{kl} = B_{\text{s}}\tilde{b}_{ij} + \frac{B_{\text{b}}}{2}\text{Tr}(b)\delta_{ij} + B_{\text{o}}\tilde{b}^{\text{o}}_{ij}, \quad
\tag{B3}
$$

where

$$
\text{Tr}(b) = b_{jj}, \quad \tilde{b}_{ij} = \frac{1}{2}(b_{ij} + b_{ji}) - \frac{1}{2}b_{kk}\delta_{ij}, \quad \tilde{b}^{\text{o}}_{ij} = \varepsilon_{ik}\tilde{b}_{kj}.
\tag{B4}
$$

One important relation that is used in Appendix A is

$$
\underline{\underline{a}} : \boldsymbol{A} : \underline{\underline{a}} = A_{\text{s}}(\tilde{a}_{ij})^2 + \frac{1}{2}A_{\text{b}}(\text{Tr}(a))^2,
\tag{B5}
$$

where we see that the odd contribution drops out due to its antisymmetric nature. Consistently with the definition (B3), we define the contraction $\boldsymbol{C} = \boldsymbol{AB}$ of two tensors $\boldsymbol{A}$ and $\boldsymbol{B}$ in terms of their components as

$$
C_{ijkl} = A_{ijmn}B_{mnkl}.
\tag{B6}
$$

Odd isotropic rank-4 tensors form a commutative group under multiplication since

$$
\begin{aligned}
C_{ijkl} = A_{ijmn}B_{mnkl} = \frac{C_{\text{s}}}{2}(\delta_{ik}\delta_{jl} + \delta_{il}\delta_{jk} - \delta_{ij}\delta_{kl}) + \frac{C_{\text{b}}}{2}\delta_{ij}\delta_{kl} \\
+ \frac{C_{\text{o}}}{4}(\delta_{ik}\varepsilon_{jl} + \delta_{il}\varepsilon_{jk} + \delta_{jk}\varepsilon_{il} + \delta_{jl}\varepsilon_{ik}),
\end{aligned}
\tag{B7}
$$

where

$$
C_{\text{s}} = A_{\text{s}}B_{\text{s}} - A_{\text{o}}B_{\text{o}}, \quad C_{\text{b}} = A_{\text{b}}B_{\text{b}}, \quad C_{\text{o}} = A_{\text{o}}B_{\text{s}} + A_{\text{s}}B_{\text{o}},
\tag{B8}
$$

where we have used the relation $\varepsilon_{ij}\varepsilon_{kl} = \delta_{ik}\delta_{jl} - \delta_{il}\delta_{jk}$. The identity tensor $\boldsymbol{I}$ is defined componentwise as

$$
I_{ijkl} = \frac{1}{2}(\delta_{ik}\delta_{jl} + \delta_{il}\delta_{jk}),
\tag{B9}
$$

and the inverse $\boldsymbol{N} = \boldsymbol{M}^{-1}$ of $\boldsymbol{M}$ satisfies $\boldsymbol{M}^{-1}\boldsymbol{M} = \boldsymbol{M}\boldsymbol{M}^{-1} = \boldsymbol{I}$ and has the following elements:

$$
N_{\text{s}} = \frac{M_{\text{s}}}{M_{\text{s}}^2 + M_{\text{o}}^2}, \quad N_{\text{b}} = \frac{1}{M_{\text{b}}}, \quad N_{\text{o}} = -\frac{M_{\text{o}}}{M_{\text{s}}^2 + M_{\text{o}}^2}. \quad
\tag{B10}
$$

APPENDIX C: ONSAGER RELATIONS WITH ODD ISOTROPIC RANK-4 TENSORS

In this Appendix, we derive Onsager relations in the case in which the state variables $\underline{\underline{\Phi}}^{\alpha}$ of the system are rank-2 symmetric tensors. We define their conjugate forces as $\underline{\underline{f}}^{\alpha} = -\delta\mathcal{F}/\delta\underline{\underline{\Phi}}^{\alpha}$, where $\mathcal{F}[\underline{\underline{\Phi}}]$ is the free energy of the system. The time derivative of the free energy can therefore be written as

$$
\dot{\mathcal{F}} = -\sum_{\alpha}\dot{\Phi}^{\alpha}_{ij}f^{\alpha}_{ij},
\tag{C1}
$$

where the summation over repeated Latin indices is implicit, while we write explicitly the summation over Greek indices. Linear relations between thermodynamics fluxes and forces read

$$
\underline{\underline{\dot{\Phi}}}^{\alpha} = \sum_{\beta}\boldsymbol{\mathcal{L}}^{\alpha\beta} : \underline{\underline{f}}^{\beta},
\tag{C2}
$$

where each $\boldsymbol{\mathcal{L}}^{\alpha\beta}$ is an odd isotropic rank-4 tensor. Writing explicitly the components, we have

$$
\dot{\Phi}^{\alpha}_{ij} = \sum_{\beta}\mathcal{L}^{\alpha\beta}_{ijkl}f^{\beta}_{kl}.
\tag{C3}
$$

We deduce

$$
\dot{\mathcal{F}} = -\sum_{\alpha\beta}(\boldsymbol{\mathcal{L}}^{\alpha\beta} : \underline{\underline{f}}^{\beta})_{ij}f^{\alpha}_{ij} = -\sum_{\alpha\beta}\mathcal{L}^{\alpha\beta}_{ijkl}f^{\alpha}_{ij}f^{\beta}_{kl},
\tag{C4}
$$

from which we deduce that the odd part of the diagonal elements of $\boldsymbol{\mathcal{L}}$ (i.e., the coefficients $\mathcal{L}^{\alpha\alpha}_{\text{o}}$) do not contribute to the rate of change of the free energy as a consequence of Eq. (B5). We now derive the symmetries of the Onsager matrix $\boldsymbol{\mathcal{L}}^{\alpha\beta}$ under time reversal. For this purpose, we first introduce the partition function

$$
\mathcal{Z} = \int \mathcal{D}\underline{\underline{\Phi}}\, e^{-\mathcal{F}[\underline{\underline{\Phi}}]/k_B T},
\tag{C5}
$$

which can be used to compute correlation functions. We have

$$
\begin{aligned}
\langle \underline{\underline{\Phi}}^\alpha \underline{f}^\beta \rangle &= \frac{1}{\mathcal{Z}} \int \mathcal{D}\underline{\underline{\Phi}} \, \underline{\underline{\Phi}}^\alpha \, \underline{f}^\beta e^{-\mathcal{F}[\underline{\Phi}]/k_B T}, \\
&= -\frac{1}{\mathcal{Z}} \int \mathcal{D}\underline{\underline{\Phi}} \, \underline{\underline{\Phi}}^\alpha \frac{\delta F}{\delta \underline{\underline{\Phi}}^\beta} e^{-\mathcal{F}[\underline{\Phi}]/k_B T}, \\
&= \frac{k_B T}{\mathcal{Z}} \int \mathcal{D}\underline{\underline{\Phi}} \, \underline{\underline{\Phi}}^\alpha \frac{\delta}{\delta \underline{\underline{\Phi}}^\beta} e^{-\mathcal{F}[\underline{\Phi}]/k_B T}, \\
&= -\frac{k_B T}{\mathcal{Z}} \int \mathcal{D}\underline{\underline{\Phi}} \frac{\delta \underline{\underline{\Phi}}^\alpha}{\delta \underline{\underline{\Phi}}^\beta} e^{-\mathcal{F}[\underline{\Phi}]/k_B T}, \\
&= -k_B T \delta^{\alpha\beta} \boldsymbol{I}.
\end{aligned} \tag{C6}
$$

Note that the same procedure can be used to obtain relations for higher-order correlation functions. Considering for simplicity scalar quantities, we have the generic expression

$$
\begin{aligned}
\langle \phi^{\alpha_1} \cdots \phi^{\alpha_N} f^\beta \rangle = {} & -k_B T (\delta^{\alpha_1 \beta} \langle \phi^{\alpha_2} \cdots \phi^{\alpha_N} \rangle \\
& + \delta^{\alpha_2 \beta} \langle \phi^{\alpha_1} \phi^{\alpha_3} \cdots \phi^{\alpha_N} \rangle + \cdots).
\end{aligned} \tag{C7}
$$

The last equality of Eq. (C6) is best derived using indices

$$
\frac{\delta \Phi_{ij}^\alpha}{\delta \Phi_{kl}^\beta} = \frac{1}{2}(\delta_{ik}\delta_{jl} + \delta_{il}\delta_{jk})\delta^{\alpha\beta} = I_{ijkl}\delta^{\alpha\beta}, \tag{C8}
$$

where we have used the fact that the $\underline{\underline{\Phi}}^\alpha$ are symmetric tensors. The second to last equality in Eq. (C6) has been obtained using an integration by parts. The boundary terms vanish with the assumption that F diverges at infinity. Using Eqs. (C3) and (C6), we can now compute

$$
\begin{aligned}
\langle \Phi_{ij}^\alpha \dot{\Phi}_{kl}^\beta \rangle &= \langle \Phi_{ij}^\alpha \mathcal{L}_{klmn}^{\beta\gamma} f_{mn}^\gamma \rangle, \\
&= \mathcal{L}_{klmn}^{\beta\gamma} \langle \Phi_{ij}^\alpha f_{mn}^\gamma \rangle, \\
&= -k_B T \mathcal{L}_{klij}^{\beta\alpha}.
\end{aligned} \tag{C9}
$$

The same correlation function can also be computed using time reversal. We have

$$
\begin{aligned}
\langle \underline{\underline{\Phi}}^\alpha \underline{\underline{\dot{\Phi}}}^\beta \rangle &= \lim_{\Delta \to 0} \frac{1}{\Delta t}(\langle \underline{\underline{\Phi}}^\alpha(t)\underline{\underline{\Phi}}^\beta(t+\Delta t)\rangle - \langle \underline{\underline{\Phi}}^\alpha(t)\underline{\underline{\Phi}}^\beta(t)\rangle), \\
&= \lim_{\Delta t \to 0} \frac{1}{\Delta t}(\langle \underline{\underline{\Phi}}^\alpha(t-\Delta t)\underline{\underline{\Phi}}^\beta(t)\rangle - \langle \underline{\underline{\Phi}}^\alpha(t)\underline{\underline{\Phi}}^\beta(t)\rangle), \\
&= \lim_{\Delta t \to 0} \frac{\epsilon^\alpha \epsilon^\beta}{\Delta t}(\overline{\langle \underline{\underline{\Phi}}^\alpha(-t+\Delta t)\underline{\underline{\Phi}}^\beta(-t)\rangle} \\
&\quad - \overline{\langle \underline{\underline{\Phi}}^\alpha(-t)\underline{\underline{\Phi}}^\beta(-t)\rangle}), \\
&= \lim_{\Delta t \to 0} \frac{\epsilon^\alpha \epsilon^\beta}{\Delta t}(\overline{\langle \underline{\underline{\Phi}}^\alpha(t+\Delta t)\underline{\underline{\Phi}}^\beta(t)\rangle} - \overline{\langle \underline{\underline{\Phi}}^\alpha(t)\underline{\underline{\Phi}}^\beta(t)\rangle}), \\
&= \epsilon^\alpha \epsilon^\beta \overline{\langle \underline{\underline{\dot{\Phi}}}^\alpha \underline{\underline{\Phi}}^\beta \rangle},
\end{aligned} \tag{C10}
$$

where ϵ^α is the signature of $\underline{\underline{\Phi}}^\alpha$ under time reversal, and the overline $\overline{\cdots}$ indicates that the sign of some parameters (for instance magnetic field) has to be changed. We thus deduce the Onsager matrix symmetry:

$$
\mathcal{L}_{ijkl}^{\alpha\beta} = \epsilon^\alpha \epsilon^\beta \overline{\mathcal{L}}_{klij}^{\beta\alpha}. \tag{C11}
$$

It yields in particular

$$
\mathcal{L}_{ijkl}^{\alpha\alpha} = \overline{\mathcal{L}}_{klij}^{\alpha\alpha}, \tag{C12}
$$

which means that an equilibrium odd viscosity needs to change sign under time reversal to be nonvanishing. This is consistent, for instance, with odd viscosity [6,57–59], which is proportional to the magnetic field and therefore changes sign upon time reversal. Assuming a sign change upon time reversal for all odd coefficients thus leads to the following structure for the Onsager matrix:

$$
\boldsymbol{\mathcal{L}}^{\alpha\beta} = \begin{pmatrix} \boldsymbol{\eta}^{\mathrm{p}} & -\boldsymbol{\nu}^{\mathrm{p}} \\ \boldsymbol{\nu}^{\mathrm{p}} & \boldsymbol{\gamma}^{\mathrm{p}} \end{pmatrix}^{\alpha\beta}, \tag{C13}
$$

where $\boldsymbol{\eta}^{\mathrm{p}}$, $\boldsymbol{\nu}^{\mathrm{p}}$, and $\boldsymbol{\gamma}^{\mathrm{p}}$ are isotropic rank-4 tensors that include odd and even parts. This yields Eq. (A9).

APPENDIX D: SHELL LOCALIZATION

In this Appendix, we explain how shell localization is used to obtain the response matrix of Eq. (16). For this, we first invert Eq. (14) as

$$
v_i(\mathbf{k}, s) = \mathcal{G}_{ij}^{-1}(\mathbf{k}, s) f_j^{\mathrm{ext}}(\mathbf{k}, s). \tag{D1}
$$

Equation (D1) gives the velocity induced by a force for a given Fourier wave vector and Laplace frequency. We then consider the force applied on a probe particle, which is a rigid disk of radius a located at the origin. Due to the rotational symmetry of the disk, we can decompose the force density as

$$
f_j^{\mathrm{ext}}(s, \mathbf{k}) = L(k) F_j(s). \tag{D2}
$$

The shell localization method amounts to assuming that the force density is uniformly localized on the surface of the probe particle [49,61,62], i.e.,

$$
L(\mathbf{x}) = \frac{1}{2\pi a}\delta(|\mathbf{x}| - a). \tag{D3}
$$

The assumption of a uniform distribution in real space has been found to give consistent results for systems where no-slip boundary conditions apply [39,49,50]. Fourier transforming Eq. (D3) yields

$$
L(k) = J_0(ak), \tag{D4}
$$

with $J_0(z)$ the zeroth Bessel function of the first kind. To obtain the bead velocity, we must inverse Fourier transform Eq. (D1) to obtain the fluid velocity in real space, which is coupled to the probe particle velocity through no-slip boundary conditions. The most accurate way to do this would be to relate the probe particle velocity $U_i(s)$ to $v_i(|\mathbf{x}| = a, s)$, which can be done averaging over the boundary line between the fluid and the probe particle [50]. We instead consider the fluid velocity localized at $|\mathbf{x}| = 0$, i.e., we relate

$$
U_i(s) = v_i(|\mathbf{x}| = 0, s), \tag{D5}
$$

as has also been done in Refs. [39,49,61]. As shown in Ref. [50], averaging over velocities at $|x| = a$ would yield an additional factor $J_0(ak)$ in the integrand of Eq. (16). However, this modification only leads to minor quantitative effects, and thus we ignore it for mathematical simplicity.

APPENDIX E: COMPUTING THE PROBE PARTICLE STABILITY FOR ACTIVE ODD FLUIDS

1. General case

In this Appendix, we detail the stability analysis of a probe particle in an active odd viscoelastic fluid, as discussed in Sec. III. Such stability is determined by the long-term velocity of the probe particle. This velocity follows from Eq. (12), which can be rewritten as

$$U_i(t) = \frac{1}{2i\pi} \int_{\Gamma-i\infty}^{\Gamma+i\infty} ds\, e^{st} \int \frac{d^2\mathbf{k}}{(2\pi)^2} \mathcal{M}_{ij}(\mathbf{k}, s) L(k) F_j(s),$$
(E1)

where Γ is a real number so that the contour path of integration is in the region of convergence of the integrand. As discussed in the main text, we consider a force perturbation along the eigendirections of $\mathcal{M}_{ij}$, and furthermore we consider an instantaneous perturbation applied at $t = 0$, such that $F_j(t) \propto \delta(t)$, or $F_j(s) \propto 1$ in Laplace space. The velocity of the probe after this initial perturbation is thus given by

$$U_i(t) = \frac{1}{2\pi i} \int_{\Gamma-i\infty}^{\Gamma+i\infty} ds\, e^{st} \int \frac{d^2\mathbf{k}}{(2\pi)^2} m_i(\mathbf{k}, s) L(k),$$
(E2)

where $m_i(\mathbf{k}, s)$ depends on the eigenvalues of $\mathcal{M}_{ij}$ and on the form of the initial perturbation. We will not focus on its precise expression in the following discussion, but the crucial point is that $m_i(\mathbf{k}, s)$ is a rational fraction in s. This implies that the inverse Laplace transform can be computed as

$$U_i(t) = \sum_\ell \int \frac{d^2\mathbf{k}}{(2\pi)^2} m_{i,\ell}(\mathbf{k}) L(k)\, e^{s_\ell^*(\mathbf{k})t},$$
(E3)

where the $s_\ell^*(\mathbf{k})$ are the poles in s of the rational fraction m_i and where the $m_{i,\ell}(\mathbf{k})$ are the residues of m_i at $s = s_\ell^*(\mathbf{k})$. As a consequence of this simple form, a sufficient condition for the long-time stability of the probe is directly given by the sign of the real part of the poles of m_i:

$$\text{Re}(s_\ell^*(\mathbf{k})) \leqslant 0 \qquad \forall\ell,\ \forall\mathbf{k},$$
(E4)

which is the condition given in the main text.

2. Incompressible limit

To continue our analysis while keeping the technicalities to a minimum, we now restrict ourselves to the incompressible case. In this simpler case, $\mathcal{M}_{ij}$ is proportional to the identity tensor, such that the probe velocity can be written as

$$U_i(t) = \frac{1}{2i\pi} \int_{\Gamma-i\infty}^{\Gamma+i\infty} ds\, e^{st} \int_0^\infty \frac{dk}{2\pi} r(k, s) F_i(s),$$
(E5)

where we have defined

$$r(k, s) = \frac{1}{4\pi \eta_s} \frac{ak J_0(ak)}{\tau_0 s + (ak)^2 A_s(s)/\eta_s},$$
(E6)

with $\tau_0 = \rho_0 a^2/\eta_s$, and we only consider instantaneous perturbations [$F_i(s)$ constant]. As discussed in the previous section, the long-time stability is then given by the poles in s of r. They correspond to the roots of the third-order

polynomial $P(s) = s^3 + a_2 s^2 + a_1 s + a_0$ with

$$a_2 = (ak)^2/\tau_0 + 4\gamma_s G_s,$$

$$a_1 = G_s\left[4G_s(\gamma_o^2 + \gamma_s^2) + \frac{(ak)^2}{\tau_0 \eta_s}(4\gamma_s \eta_s - \nu_o^2 + \nu_s^2)\right],$$

$$a_0 = \frac{2G_s^2(ak)^2}{\tau_0 \eta_s}\left[2\eta_s \gamma_o^2 + 2\gamma_o \nu_o \nu_s + \gamma_s(2\gamma_s \eta_s - \nu_o^2 + \nu_s^2)\right],$$
(E7)

where we have considered the case $\nu'_{s,o} = \nu_{s,o}$. The roots $s_\ell^*(k)$ of $P(s)$ all have negative real parts iff $a_{0,1,2} > 0$ and $a_2 a_1 - a_0 > 0$ according to the Routh-Hurwitz stability criterion. We note that a_2 is always positive. The conditions $a_{0,1} > 0$ are equivalent to

$$4\gamma_s \eta_s - \nu_o^2 + \nu_s^2 > 0,$$
(E8a)

$$2\eta_s \gamma_o^2 + 2\gamma_o \nu_o \nu_s + \gamma_s(2\gamma_s \eta_s - \nu_o^2 + \nu_s^2) > 0.$$
(E8b)

The condition $a_2 a_1 - a_0 > 0$ takes the form of a second-order polynomial $Q(X) = b_2 X^2 + b_1 X + b_0$ with $X = (ak)^2$ and $b_0 = 8G_s^3 \gamma_s(\gamma_s^2 + \gamma_o^2)$, $b_1 = G_s^2[\gamma_s(8\gamma_s \eta_s - \nu_o^2 + \nu_s^2) - 2\gamma_o \nu_o \nu_s]/(\tau_0 \eta_s)$, $b_2 = G_s(4\gamma_s \eta_s - \nu_o^2 + \nu_s^2)/(2\tau_0^2 \eta_s)$. With $\Delta = b_1^2 - 4b_0 b_2$ the discriminant of Q, the condition $a_2 a_1 - a_0 > 0$ thus translates to

$$\Delta < 0 \text{ or } \begin{cases} \Delta \geqslant 0 \quad \text{and} \\ \gamma_s(\nu_s^2 - \nu_o^2) - 2\gamma_o \nu_o \nu_s + 8\eta_s \gamma_s^2 < 0. \end{cases}$$
(E8c)

A similar analysis can be conducted for $\nu'_{s,o} \neq \nu_{s,o}$.

APPENDIX F: INVERSE LAPLACE TRANSFORM IN THE INCOMPRESSIBLE CASE

In this Appendix, we compute explicitly the velocity of a probe immersed in an odd incompressible viscoelastic fluid. In the incompressible limit, the probe velocity $U_i(t)$ is directly obtained as the inverse Laplace transform of the complex velocity $U_i(s)$:

$$U_i(t) = \frac{1}{2i\pi} \int_{\Gamma-i\infty}^{\Gamma+i\infty} ds\, e^{st} U_i(s),$$
(F1a)

where $U_i(s)$ was obtained in Eq. (24), and we rewrite it here for convenience:

$$U_i(s) = \frac{K_0\left(\sqrt{\frac{s\tau_0}{A_s(s)/\eta_s}}\right)}{4\pi A_s(s)} F_i(s).$$
(F1b)

As we will see in the following, the computation of the inverse Laplace transform requires performing contour integration in the complex plane, which has to be carefully designed due to the presence of the square root in Eq. (F1b). Therefore, in order to simplify the following discussion, we consider the case in which the coefficient γ_o vanishes, although a similar result can be obtained in the general case. For $\gamma_o = 0$, the complex viscosity A_s reads

$$A_s(s) = \eta_s \frac{s - s_1}{s - s_2},$$
(F2)

where $s_1 = -G_s(2\eta_s \gamma_s - \nu_o^2 + \nu_s^2)/\eta_s$ and $s_2 = -2\gamma_s G_s$. Note that $s_2 < 0$ while s_1 can be either sign, and it is positive
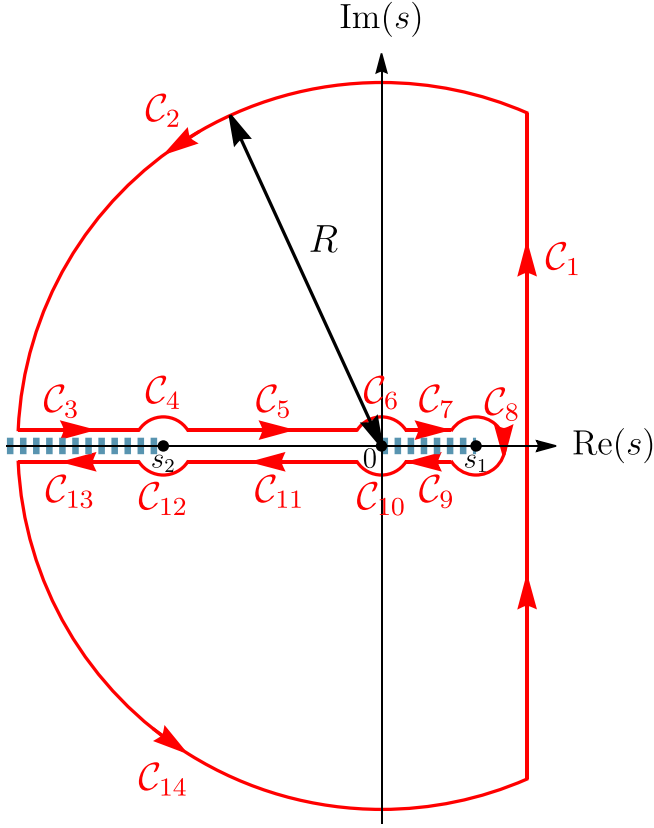
FIG. 6. Contour integration in the complex plane used to compute the inverse Laplace transform (F3). The dashed blue lines along the real axis indicate branch cuts of the integrand. To compute the integrals G_i along the contours $\mathcal{C}_i$, the radius of the large circle R and the width 2ε between the segments above and below the real axis are sent to ∞ and 0, respectively.

in the unstable regime according to Eq. (21b). In the following, we consider the unstable case and have $s_2 < 0 < s_1$. We also introduce $\Delta s = s_2 - s_1 < 0$ for convenience. The computation in the stable case ($s_1 < 0$) follows the same steps.

Finally, we consider the velocity after an instantaneous force is applied. We thus take $F_j(t) \propto \delta(t)$ [or $F_j(s) \propto 1$ in Laplace space], and the drag response defined in Eq. (23) reads

$$
\eta_s M_\parallel(t) = \frac{1}{4\pi} \int_{\Gamma - i\infty}^{\Gamma + i\infty} \frac{ds}{2i\pi} g(s) e^{st},
$$

$$
g(s) = \frac{s - s_2}{s - s_1} K_0 \left(\sqrt{\frac{s(s - s_2)}{s - s_1}} \right). \tag{F3}
$$

This inverse Laplace transform can be computed using residues. We first note that the function $g(s)$ has branch cuts for $\mathrm{Re}[s(s - s_2)/(s - s_1)] < 0$, that is, for $\mathrm{Re}(s) < s_2$ and $0 < \mathrm{Re}(s) < s_1$, and is analytic otherwise. We thus define a closed integration contour (see Fig. 6) that avoids the branch cuts such that $\sum_i G_i = 0$, where $G_i = \int_{\mathcal{C}_i} ds\, g(s) e^{st}/(2i\pi)$. In the following, we detail the computation of $G_{i>1}$.

Contours $\mathcal{C}_2$ and $\mathcal{C}_{14}$. We set $s = Re^{i\theta}$ with $\theta \in [\pi/2, \pi]$ such that

$$
G_2 = \lim_{R \to \infty} \frac{1}{2i\pi} \int_{\pi/2}^{\pi} d\theta\, iRe^{i\theta} \frac{Re^{i\theta} - s_2}{Re^{i\theta} - s_1}
$$

$$
\times K_0 \left(\sqrt{R} e^{i\theta/2} \sqrt{\frac{Re^{i\theta} - s_2}{Re^{i\theta} - s_1}} \right) e^{Re^{i\theta} t}, \tag{F4}
$$

which vanishes in the limit $R \to \infty$ because of the last exponential factor in the above equation with real part $Rt \cos\theta \leqslant 0$ (for $t > 0$ and $\theta \in [\pi/2, \pi]$). Similarly, we find $G_{14} = 0$.

Contours $\mathcal{C}_3$ and $\mathcal{C}_{13}$. For $\mathcal{C}_3$, we set $s = s_2 + e^{i\pi} u$ with $u \in [0, \infty[$, from which we obtain

$$
G_3 = \frac{1}{2i\pi} \int_{\infty}^{0} du\, e^{i\pi} \frac{e^{i\pi} u}{e^{i\pi} u + s_2 - s_1}
$$

$$
\times K_0 \left(\sqrt{\frac{(e^{i\pi} u + s_2) e^{i\pi} u}{e^{i\pi} u + s_2 - s_1}} \right) e^{(s_2 + e^{i\pi} u) t},
$$

$$
= \frac{1}{2i\pi} \int_{0}^{\infty} du\, \frac{u}{u - \Delta s} K_0 \left(i\sqrt{u} \sqrt{\frac{(u - s_2)}{u - \Delta s}} \right) e^{s_2 t} e^{-ut}. \tag{F5}
$$

Similarly, setting $s = s_2 + e^{-i\pi} u$ along $\mathcal{C}_{13}$ yields

$$
G_{13} = -\frac{1}{2i\pi} \int_{0}^{\infty} du\, \frac{u}{u - \Delta s} K_0 \left(-i\sqrt{u} \sqrt{\frac{(u - s_2)}{u - \Delta s}} \right) e^{s_2 t} e^{-ut}. \tag{F6}
$$

Contours $\mathcal{C}_4$ and $\mathcal{C}_{12}$. For $\mathcal{C}_4$, we set $s = s_2 + \varepsilon e^{i\phi}$ with $\phi \in [0, \pi]$, from which we obtain

$$
G_4 = \lim_{\varepsilon \to 0} \frac{1}{2i\pi} \int_{\pi}^{0} d\phi\, \varepsilon i e^{i\phi} \frac{\varepsilon e^{i\phi}}{\varepsilon e^{i\phi} + \Delta s}
$$

$$
\times K_0 \left(\sqrt{\varepsilon} e^{i\phi/2} \sqrt{\frac{e^{i\pi} \varepsilon + s_2}{e^{i\pi} \varepsilon - s_1}} \right) e^{(s_2 + \varepsilon e^{i\phi}) t},
$$

$$
= \lim_{\varepsilon \to 0} \frac{1}{2i\pi} \int_{\pi}^{0} d\phi\, \frac{\varepsilon^2}{\Delta s} K_0 \left(\sqrt{\varepsilon} e^{i\phi/2} \sqrt{\frac{s_2}{-s_1}} \right) e^{s_2 t}, \tag{F7}
$$

which vanishes in the limit $\varepsilon \to 0$ since $K_0(x) \underset{x \to 0}{\sim} -\log x$. Similar steps yield $G_{12} = 0$.

Contours $\mathcal{C}_5$ and $\mathcal{C}_{11}$. The contributions stemming from $\mathcal{C}_4$ and $\mathcal{C}_{11}$ cancel each other, since they correspond to an integration in both directions of a holomorphic function along these contours.

Contours $\mathcal{C}_6$ and $\mathcal{C}_{10}$. For $\mathcal{C}_6$, we set $s = \varepsilon e^{i\phi}$ with $\phi \in [0, \pi]$, from which a computation similar of that of G_4 yields

$$
G_5 = \lim_{\varepsilon \to 0} \frac{1}{2i\pi} \int_{\pi}^{0} d\phi\, \frac{s_2}{s_1} \varepsilon K_0 \left(\sqrt{\varepsilon} e^{i\phi/2} \sqrt{\frac{s_2}{s_1}} \right), \tag{F8}
$$

which vanishes in the limit $\varepsilon \to 0$. Similar steps yield $G_{10} = 0$.

Contours $\mathcal{C}_7$ *and* $\mathcal{C}_9$. For $\mathcal{C}_7$, we set $s = s_1 + s_1 u e^{i\pi}$ with $v \in [0, 1]$, from which we obtain

$$G_7 = \frac{1}{2i\pi} \int_0^1 dv \, \frac{\Delta s + s_1 v}{v}$$
$$\times K_0 \left(e^{-i\pi/2} \sqrt{\frac{(v-1)(s_1 v + \Delta s)}{v}} \right) e^{s_1(1-v)t}. \quad \text{(F9)}$$

Similarly, setting $s = s_2 + e^{-i\pi} u$ along $\mathcal{C}_{13}$ yields

$$G_9 = -\frac{1}{2i\pi} \int_0^1 dv \, \frac{\Delta s + s_1 v}{v}$$
$$\times K_0 \left(e^{+i\pi/2} \sqrt{\frac{(v-1)(s_1 v + \Delta s)}{v}} \right) e^{s_1(1-v)t}. \quad \text{(F10)}$$

Contour $\mathcal{C}_8$. We set $s = s_1 + \varepsilon e^{i\phi}$ with $\phi \in [-\pi, \pi]$, from which we obtain

$$G_8 = \lim_{\varepsilon \to 0} \frac{1}{2i\pi} \int_\pi^{-\pi} d\phi \, (-\Delta s) K_0 \left(\frac{1}{\sqrt{\varepsilon}} e^{i\phi/2} \sqrt{s_1(-\Delta s)} \right) e^{s_1 t}, \quad \text{(F11)}$$

which vanishes in the limit $\varepsilon \to 0$ since $K_0(x) \underset{x \to \infty}{\sim} -\sqrt{\pi/(2x)} \, e^{-x}$.

Since $\eta_s M_\parallel(t) = G_1/(4\pi)$ and $G_1 = -\sum_{i>1} G_i = -(G_3 + G_{13} + G_7 + G_9)$, we finally obtain

$$\eta_s M_\parallel(t) = \frac{1}{8\pi} \left[\int_0^\infty du \, a(u, t) + \int_0^1 dv \, b(v, t) \right] \quad \text{(F12a)}$$

with

$$a(u, t) = \frac{u}{u - \Delta s} J_0 \left(\sqrt{\frac{u(u - s_2)}{u - \Delta s}} \right) e^{s_2 t - ut}, \quad \text{(F12b)}$$

$$b(v, t) = \frac{\Delta s + s_1 v}{-v} J_0 \left(\sqrt{\frac{(v-1)(s_1 v + \Delta s)}{v}} \right) e^{s_1(1-v)t}, \quad \text{(F12c)}$$

and where we have used the identities $K_0(ix) - K_0(-ix) = -i\pi J_0(x)$ for $x > 0$. Importantly, we verify that in the long-time limit, the behavior of $M_\parallel(t) \underset{t \to \infty}{\sim} e^{s_1 t}$ is set by the real part of s_1 [since $(s_2 - u)t$ is always negative], and thus it diverges, as expected for our choice $s_1 > 0$.

[1] J. M. Epstein and K. K. Mandadapu, Time-reversal symmetry breaking in two-dimensional nonequilibrium viscous fluids, Phys. Rev. E **101**, 052614 (2020).

[2] C. Hargus, K. Klymko, J. M. Epstein, and K. K. Mandadapu, Time reversal symmetry breaking and odd viscosity in active fluids: Green–Kubo and NEMD results, J. Chem. Phys. **152**, 201102 (2020).

[3] R. Lier, J. Armas, S. Bo, C. Duclut, F. Jülicher, and P. Surówka, Passive odd viscoelasticity, Phys. Rev. E **105**, 054607 (2022).

[4] M. Han, M. Fruchart, C. Scheibner, S. Vaikuntanathan, J. J. de Pablo, and V. Vitelli, Fluctuating hydrodynamics of chiral active fluids, Nat. Phys. **17**, 1260 (2021).

[5] C. Hargus, J. M. Epstein, and K. K. Mandadapu, Odd diffusivity of chiral random motion, Phys. Rev. Lett. **127**, 178001 (2021).

[6] V. Soni, E. S. Bililign, S. Magkiriadou, S. Sacanna, D. Bartolo, M. J. Shelley, and W. T. M. Irvine, The odd free surface flows of a colloidal chiral fluid, Nat. Phys. **15**, 1188 (2019).

[7] C. Reichhardt and C. J. O. Reichhardt, Active microrheology, Hall effect, and jamming in chiral fluids, Phys. Rev. E **100**, 012604 (2019).

[8] T. Markovich and T. C. Lubensky, Odd viscosity in active matter: Microscopic origin and 3d effects, Phys. Rev. Lett. **127**, 048001 (2021).

[9] C. J. O. Reichhardt and C. Reichhardt, Active rheology in odd-viscosity systems, Europhys. Lett. **137**, 66004 (2022).

[10] S. Fürthauer, M. Strempel, S. W. Grill, and F. Jülicher, Active chiral fluids, Eur. Phys. J. E **35**, 89 (2012).

[11] T. H. Tan, A. Mietke, J. Li, Y. Chen, H. Higinbotham, P. J. Foster, S. Gokhale, J. Dunkel, and N. Fakhri, Odd dynamics of living chiral crystals, Nature (London) **607**, 287 (2022).

[12] D. Banerjee, V. Vitelli, F. Jülicher, and P. Surówka, Active viscoelasticity of odd materials, Phys. Rev. Lett. **126**, 138001 (2021).

[13] P. Surówka, A. Souslov, F. Jülicher, and D. Banerjee, Odd cosserat elasticity in active materials, Phys. Rev. E **108**, 064609 (2023).

[14] E. Kalz, H. D. Vuijk, J.-U. Sommer, R. Metzler, and A. Sharma, Oscillatory force autocorrelations in equilibrium odd-diffusive systems, Phys. Rev. Lett. **132**, 057102 (2024).

[15] E. Kalz, H. D. Vuijk, I. Abdoli, J.-U. Sommer, H. Löwen, and A. Sharma, Collisions enhance self-diffusion in odd-diffusive systems, Phys. Rev. Lett. **129**, 090601 (2022).

[16] D. Banerjee, A. Souslov, A. G. Abanov, and V. Vitelli, Odd viscosity in chiral active fluids, Nat. Commun. **8**, 1573 (2017).

[17] A. Abanov, T. Can, and S. Ganeshan, Odd surface waves in two-dimensional incompressible fluids, SciPost Phys. **5**, 010 (2018).

[18] S. Ganeshan and A. G. Abanov, Odd viscosity in two-dimensional incompressible fluids, Phys. Rev. Fluids **2**, 094101 (2017).

[19] T. Khain, C. Scheibner, M. Fruchart, and V. Vitelli, Stokes flows in three-dimensional fluids with odd and parity-violating viscosities, J. Fluid Mech. **934**, A23 (2022).

[20] Y. Hosaka, R. Golestanian, and A. Daddi-Moussa-Ider, Hydrodynamics of an odd active surfer in a chiral fluid, New J. Phys. **25**, 083046 (2023).

[21] Y. Hosaka, S. Komura, and D. Andelman, Hydrodynamic lift of a two-dimensional liquid domain with odd viscosity, Phys. Rev. E **104**, 064613 (2021).

[22] Y. Hosaka, D. Andelman, and S. Komura, Pair dynamics of active force dipoles in an odd-viscous fluid, Eur. Phys. J. E **46**, 18 (2023).

[23] C. Scheibner, A. Souslov, D. Banerjee, P. Surówka, W. T. M. Irvine, and V. Vitelli, Odd elasticity, Nat. Phys. **16**, 475 (2020).

[24] L. Braverman, C. Scheibner, B. Van Saders, and V. Vitelli, Topological defects in solids with odd elasticity, Phys. Rev. Lett. **127**, 268001 (2021).

[25] C. Floyd, A. R. Dinner, and S. Vaikuntanathan, Pattern formation in odd viscoelastic fluids, arXiv:2210.01159.

[26] M. Fruchart, M. Han, C. Scheibner, and V. Vitelli, The odd ideal gas: Hall viscosity and thermal conductivity from non-Hermitian kinetic theory, arXiv:2202.02037.

[27] Z. Liao, W. T. M. Irvine, and S. Vaikuntanathan, Rectification in nonequilibrium parity violating metamaterials, Phys. Rev. X **10**, 021036 (2020).

[28] F. M. D. Pellegrino, I. Torre, and M. Polini, Nonlocal transport and the Hall viscosity of two-dimensional hydrodynamic electron liquids, Phys. Rev. B **96**, 195401 (2017).

[29] B. N. Narozhny and M. Schütt, Magnetohydrodynamics in graphene: Shear and Hall viscosities, Phys. Rev. B **100**, 035125 (2019).

[30] A. I. Berdyugin, S. G. Xu, F. M. D. Pellegrino, R. Krishna Kumar, A. Principi, I. Torre, M. Ben Shalom, T. Taniguchi, K. Watanabe, I. V. Grigorieva, M. Polini, A. K. Geim, and D. A. Bandurin, Measuring Hall viscosity of graphene's electron fluid, Science **364**, 162 (2019).

[31] M. Fossati, C. Scheibner, M. Fruchart, and V. Vitelli, Odd elasticity and topological waves in active surfaces, arXiv:2210.03669.

[32] R. Green, J. Armas, J. de Boer, and L. Giomi, Topological waves in passive and active fluids on curved surfaces: A unified picture, arXiv:2011.12271.

[33] A. Souslov, K. Dasbiswas, M. Fruchart, S. Vaikuntanathan, and V. Vitelli, Topological waves in fluids with odd viscosity, Phys. Rev. Lett. **122**, 128001 (2019).

[34] C. Tauber, P. Delplace, and A. Venaille, A bulk-interface correspondence for equatorial waves, J. Fluid Mech. **868**, R2 (2019).

[35] E. S. Bililign, F. B. Usabiaga, Y. A. Ganan, A. Poncet, V. Soni, S. Magkiriadou, M. J. Shelley, D. Bartolo, and W. T. Irvine, Motile dislocations knead odd crystals into whorls, Nat. Phys. **18**, 212 (2022).

[36] T. G. Mason and D. A. Weitz, Optical measurements of frequency-dependent linear viscoelastic moduli of complex fluids, Phys. Rev. Lett. **74**, 1250 (1995).

[37] F. C. MacKintosh and C. F. Schmidt, Microrheology, Curr. Opin. Colloid Interface Sci. **4**, 300 (1999).

[38] T. M. Squires and T. G. Mason, Fluid mechanics of microrheology, Annu. Rev. Fluid Mech. **42**, 413 (2010).

[39] R. Lier, C. Duclut, S. Bo, J. Armas, F. Jülicher, and P. Surówka, Lift force in odd compressible fluids, Phys. Rev. E **108**, L023101 (2023).

[40] Y. Hosaka, S. Komura, and D. Andelman, Nonreciprocal response of a two-dimensional fluid with odd viscosity, Phys. Rev. E **103**, 042610 (2021).

[41] M. Gardel, M. Valentine, and D. Weitz, Microrheology, in *Microscale Diagnostic Techniques*, edited by K. S. Breuer (Springer, Berlin, 2005), pp. 1–49.

[42] R. Di Leonardo, L. Angelani, D. Dell'Arciprete, G. Ruocco, V. Iebba, S. Schippa, M. P. Conte, F. Mecarini, F. De Angelis, and E. Di Fabrizio, Bacterial ratchet motors, Proc. Natl. Acad. Sci. USA **107**, 9541 (2010).

[43] J. E. Avron, Odd Viscosity, J. Stat. Phys. **92**, 543 (1998).

[44] R. Lier, Slip-induced odd viscous flow past a cylinder, arXiv:2402.02628.

[45] A. C. Callan-Jones and F. Jülicher, Hydrodynamics of active permeating gels, New J. Phys. **13**, 093027 (2011).

[46] F. Jülicher, S. W. Grill, and G. Salbreux, Hydrodynamic theory of active matter, Rep. Prog. Phys. **81**, 076601 (2018).

[47] Y. L. Raikher, V. V. Rusakov, and R. Perzynski, Brownian motion in a viscoelastic medium modelled by a jeffreys fluid, Soft Matter **9**, 10857 (2013).

[48] P. Oswald, *Rheophysics: The Deformation and Flow of Matter* (Cambridge University Press, Cambridge, 2009).

[49] A. J. Levine and T. C. Lubensky, Response function of a sphere in a viscoelastic two-fluid medium, Phys. Rev. E **63**, 041510 (2001).

[50] A. J. Weisenborn and P. Mazur, The Oseen drag on a circular cylinder revisited, Physica A **123**, 191 (1984).

[51] J. Veysey and N. Goldenfeld, Simple viscous flows: From boundary layers to the renormalization group, Rev. Mod. Phys. **79**, 883 (2007).

[52] G. J. Elfring, L. G. Leal, and T. M. Squires, Surface viscosity and Marangoni stresses at surfactant laden interfaces, J. Fluid Mech. **792**, 712 (2016).

[53] H. A. Stone, A simple derivation of the time-dependent convective-diffusion equation for surfactant transport along a deforming interface, Phys. Fluids **2**, 111 (1990).

[54] M. Fukuma and Y. Sakatani, Relativistic viscoelastic fluid mechanics, Phys. Rev. E **84**, 026316 (2011).

[55] T. Azeyanagi, M. Fukuma, H. Kawai, and K. Yoshida, Universal description of viscoelasticity with foliation preserving diffeomorphisms, Phys. Lett. B **681**, 290 (2009).

[56] G. Salbreux and F. Jülicher, Mechanics of active surfaces, Phys. Rev. E **96**, 032404 (2017).

[57] J. E. Avron, R. Seiler, and P. G. Zograf, Viscosity of quantum Hall fluids, Phys. Rev. Lett. **75**, 697 (1995).

[58] P. Lévay, Berry phases for Landau Hamiltonians on deformed tori, J. Math. Phys. **36**, 2792 (1995).

[59] K. Jensen, M. Kaminski, P. Kovtun, R. Meyer, A. Ritz, and A. Yarom, Parity-violating hydrodynamics in $2 + 1$ dimensions, J. High Energy Phys. 05 (2012) 102.

[60] D. T. Son, Chiral metric hydrodynamics, kelvin circulation theorem, and the fractional quantum hall effect, arXiv:1907.07187.

[61] B. A. Camley and F. L. H. Brown, Beyond the creeping viscous flow limit for lipid bilayer membranes: Theory of single-particle microrheology, domain flicker spectroscopy, and long-time tails, Phys. Rev. E **84**, 021904 (2011).

[62] F. C. MacKintosh and T. C. Lubensky, Orientational order, topology, and vesicle shapes, Phys. Rev. Lett. **67**, 1169 (1991).